Regular Article

Differentiation of Human Induced Pluripotent Stem Cells into Functional Enterocyte-like Cells Using a Simple Method

Takahiro Iwao[1], Masashi Toyota[2], Yoshitaka Miyagawa[3], Hajime Okita[3], Nobutaka Kiyokawa[3], Hidenori Akutsu[2], Akihiro Umezawa[2], Kiyoshi Nagata[4] and Tamihide Matsunaga[1],*

[1]Department of Clinical Pharmacy, Graduate School of Pharmaceutical Sciences,
Nagoya City University, Nagoya, Japan
[2]Department of Reproductive Biology, National Research Institute
for Child Health and Development, Tokyo, Japan
[3]Department of Hematology and Oncology Research, National Research Institute
for Child Health and Development, Tokyo, Japan
[4]Department of Environmental and Health Science, Tohoku Pharmaceutical University, Sendai, Japan

Full text of this paper is available at http://www.jstage.jst.go.jp/browse/dmpk

Summary: Human induced pluripotent stem (iPS) cells were differentiated into the endoderm using activin A and were then treated with fibroblast growth factor 2 (FGF2) for differentiation into intestinal stem cell-like cells. These immature cells were then differentiated into enterocyte-like cells using epidermal growth factor (EGF) in 2% fetal bovine serum (FBS). At the early stage of differentiation, mRNA expression of caudal type homeobox 2 (CDX2), a major transcription factor related to intestinal development and differentiation, and leucine-rich repeat-containing G-protein-coupled receptor 5 (LGR5), an intestinal stem cell marker, was markedly increased by treatment with FGF2. When cells were cultured in medium containing EGF and a low concentration of FBS, mRNAs of specific markers of intestinal epithelial cells, including sucrase–isomaltase, the intestinal oligopeptide transporter SLC15A1/peptide transporter 1 (PEPT1), and the major metabolizing enzyme CYP3A4, were expressed. In addition, sucrase–isomaltase protein expression and uptake of β-Ala-Lys-N-7-amino-4-methylcoumarin-3-acetic acid (β-Ala-Lys-AMCA), a fluorescence-labeled substrate of the oligopeptide transporter, were detected. These results demonstrate a simple and direct method for differentiating human iPS cells into functional enterocyte-like cells.

Keywords: human iPS cells; intestinal differentiation; enterocytes; pharmacokinetics; drug metabolizing enzymes; drug transporters

Introduction

The small intestine and liver play important roles in all aspects of pharmacokinetics, including drug disposition, drug metabolism, drug transport, drug interactions, and bioavailability. Because drug-metabolizing enzymes such as cytochrome P450 (CYP) and UDP-glucuronyltransferase (UGT) and drug transporters such as ATP-binding cassette (ABC) and solute carrier (SLC) transporters are appreciably expressed in the small intestinal epithelia,[1,2] it is necessary to estimate intestinal metabolism and absorption during the early stages of drug development. To this end, various *in vivo* and *in vitro* systems have been employed to assess the intestinal

first-pass effect. However, extrapolation of experimental animal data to humans is often hampered by species differences, and primary human intestinal cells are rarely available. Therefore, a system that accurately and easily estimates intestinal membrane permeability and metabolism is urgently required.

Human induced pluripotent stem (iPS) cells can be generated by transducing reprogramming factors (OCT3/4, SOX2, KLF4, c-MYC) into somatic cells[3] and these cells share many characteristics of embryonic stem (ES) cells.[4] Human iPS cells are expected to be useful not only in regenerative medicine but also in pharmacokinetic and toxicokinetic drug development studies because their use is not as ethically regulated as that of human ES cells.

Therefore, human iPS cells have been differentiated into various cell types, including pancreatic cells,[5,6] neuron cells,[7] cardiomyocytes,[8] and hepatocytes.[9–13]

A few studies report the differentiation of iPS cells into enterocytes. In particular, mouse iPS cells were differentiated into a gut-like organ following the formation of embryoid bodies (EBs),[14] and human iPS cells were differentiated into intestinal tissue using a culture method for intestinal crypt stem cells.[15] However, functional characteristics of drug transporters and drug-metabolizing enzymes of differentiated cells are almost entirely unexplored in these reports. Thus, whether differentiated intestinal tissue or organoids can be used in drug development studies, particularly studies of the absorbability and metabolic capacity of drugs, remains unclear.

The small intestinal epithelium comprises absorptive cells, goblet cells, endocrine cells, and Paneth cells. Several signaling pathways such as Notch, Wnt, phosphoinositide 3-kinase, and bone morphogenic protein signaling are associated with intestinal development.[16] Leucine-rich repeat-containing G-protein-coupled receptor 5 (LGR5) has been identified as an intestinal stem cell marker.[17] Indeed, this was also observed in mouse LGR5-positive cells that formed a crypt–villus structure in vitro.[18] Improvements in this technique have enabled long-term culture of human epithelial cells isolated from the small intestine,[19] leading to advances in intestinal stem cell research. However, mechanisms of intestinal development are not sufficiently understood, and it is difficult to control differentiation into all four cell types.

In this study, we established a functional enterocyte-like cell line from human iPS cells for use in drug development studies. We propose a simple and direct differentiation method by two-dimensional culture. Our data may facilitate the development of an intestinal pharmacokinetic analysis system to identify safe drugs with favorable pharmacokinetic characteristics.

Materials and Methods

Materials: FGF2, FGF4, activin A, and epidermal growth factor (EGF) were purchased from PeproTech Inc. (Rocky Hill, NJ). Wnt3a was purchased from R&D Systems, Inc. (Minneapolis, MN). BD Matrigel matrix Growth Factor Reduced (Matrigel) was purchased from BD Biosciences (Bedford, MA). Affinity-isolated rabbit polyclonal antihuman sucrase–isomaltase antibody and intestinal recombinant protein epitope signature tags were purchased from Sigma-Aldrich Co. (St. Louis, MO). The purified IgG fraction of polyclonal goat antiserum against rabbit IgG conjugated with Alexa Fluor 568 and KnockOut Serum Replacement (KSR) were purchased from Invitrogen Life Technologies Co. (Carlsbad, CA). β-Ala-Lys-N-7-amino-4-methylcoumarin-3-acetic acid (β-Ala-Lys-AMCA) was purchased from BIOTREND Chemicals (Destin, FL), and (+)-(R)-trans-4-(1-aminoethyl)-N-(4-pyridyl)cyclohexanecarboxamide dihydrochloride (Y-27632) was purchased from Wako Pure Chemical Industries (Osaka, Japan). Human adult small intestine total RNA from a 66-year-old male donor was purchased from BioChain Institute Inc. (Newark, CA). Murine embryonic fibroblasts (MEFs) were obtained from Oriental Yeast Co. (Tokyo, Japan). The RNeasy Mini Kit was purchased from Qiagen (Valencia, CA). The PrimeScript RT Reagent Kit and TaKaRa SYBR Premix EX Taq II were purchased from Takara Bio Inc. (Otsu, Japan). All other reagents were of the highest quality available.

Human iPS cell cultures: A human iPS cell line (Windy) was provided by Dr. Akihiro Umezawa of the National Center for Child Health and Development. Human iPS cells were maintained in a 1:1 mixture of Dulbecco's modified Eagle's medium and Ham's nutrient mixture F-12 (DMEM/F12) containing 20% KSR, 2 mM L-glutamine, 1% MEM nonessential amino acid solution (NEAA), 0.1 mM 2-mercaptoethanol, and 5 ng/ml FGF2 at 37°C in humidified air with 5% CO_2. The human iPS cells were cultured on a feeder layer of mitomycin C-treated MEFs, and the medium was changed every day.

Differentiation into enterocyte-like cells: The human iPS cells were used for differentiation studies between passages 30 and 50. When the cells reached approximately 70% confluence, differentiation was initiated by replacing the medium with Rosewell Park Memorial Institute (RPMI) 1640 medium containing 2 mM GlutaMAX, 0.5% fetal bovine serum (FBS), 100 ng/ml activin A (a member of the transforming growth factor-β family that is known to efficiently induce differentiation into the definitive endoderm),[20,21] 100 units/ml penicillin, and 100 μg/ml streptomycin. After 48 h, the medium was replaced with RPMI 1640 containing 2 mM GlutaMAX, 2% FBS, 100 ng/ml activin A, 100 units/ml penicillin, and 100 μg/ml streptomycin, and the cells were cultured for 24 h. Subsequently, the culture medium was replaced with DMEM/F12 containing 2% FBS, 2 mM GlutaMAX, and 250 ng/ml FGF2 or FGF4 with or without 50 ng/ml Wnt3a for 96 h. The cells were then treated for 1 h with the selective Rho-associated kinase inhibitor Y-27632 at 10 μM.[22,23] The cells were then passaged on Matrigel-coated 24-well plates and cultured in DMEM/F12 containing 2% or 10% FBS, 2% B-27 supplement, 1% N2 supplement, 1% NEAA, 2 mM L-glutamine, antibiotics (100 units/ml penicillin and 100 μg/ml streptomycin), and 20 ng/ml EGF for 1, 4, 13, or 19 days. Y-27632 was added at 10 μM during the initial 24 h of culture. The medium was changed every 3 days (**Fig. 1**).

RNA extraction and reverse transcription reaction: Total RNA was isolated from differentiated iPS cells using the RNeasy Mini Kit. First-strand cDNA was prepared from 500 ng of total RNA. The reverse transcription reaction was performed using the PrimeScript RT Reagent Kit according to the manufacturer's instructions.

Real-time polymerase chain reaction (PCR) analysis: Relative mRNA expression levels were determined using SYBR Green real-time quantitative reverse transcription-PCR (RT-PCR). Real-time PCR analysis was performed on the Applied Biosystems 7300 Real Time PCR System using 7300 System SDS software version 1.4 (Applied Biosystems, Carlsbad, CA). PCR was performed with the primer pairs listed in **Table 1** using SYBR Premix EX Taq II. mRNA expression levels were normalized relative to that of the housekeeping gene glyceraldehyde-3-phosphate dehydrogenase (GAPDH).
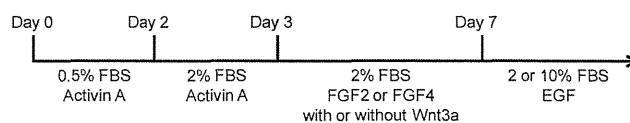

Fig. 1. Schematic of the protocol for the differentiation of human iPS cells into enterocytes
Human iPS cells were cultured in the presence of activin A (100 ng/ml) for 3 days. The cells were further cultured in medium containing FGF2 (250 ng/ml) or FGF4 (250 ng/ml) with or without Wnt3a (50 ng/ml) for 4 days. After 7 days of differentiation, the cells were treated with Y-27632 (10 μM), passaged, and subsequently cultured in the presence of 2% or 10% FBS and EGF (20 ng/ml) for 19 days.

Table 1. Sequences of primers for real-time PCR analysis

Gene name	Sense (5′→3′)	Antisense (5′→3′)	Product length (bp)
CDX2	ACCTGTGCGAGTGGATGC	TCCTTTGCTCTGCGGTTCT	232
LGR5	TGCTCTTCACCAACTGCATC	CTCAGGCTCACCAGATCCTC	193
DPP4	CAAATTGAAGCAGCCAGACA	GGAGTTGGGGAGACCCATGTA	212
Sucrase–isomaltase	GGTAAGGAGAAACCGGGAAG	GCACGTCGACCTATGGAAAT	195
Villin 1	AGCCAGATCACTGCTGAGGT	TGGACAGGTGTTCCTCCTTC	169
ISX	CAGGAAGGAAGGAAGAGCAA	TGGGTAGTGGGTAAAGTGGAA	96
CYP3A4	CTGTGTGTTTCCAAGAGAAGTTAC	TGCATCAATTTCCTCCTGCAG	298
SLC15A1/PEPT1	CACCTCCTTGAAGAAGATGGCA	GGGAAGACTGGAAGAGTTTTATCG	105
SLC46A1/PCFT	GGTCTTTGCCTTTGCCACTA	AGAGTTTAGCCCGGATGACA	98
GAPDH	GAGTCAACGGATTTGGTCGT	GACAAGCTTCCCGTTCTCAG	185

Immunofluorescence staining: The cells differentiated with FGF2 and 2% FBS were washed three times with phosphate-buffered saline (PBS) without calcium or magnesium, fixed for 30 min at room temperature in 4% paraformaldehyde, and permeabilized in PBS containing 0.1% Triton X-100 for 5 min at room temperature. After being washed three times with PBS, the cells were blocked in PBS with 2% skim milk for 20 min at room temperature and were incubated with antisucrase–isomaltase antibody diluted at 1:200 for 60 min at room temperature. Rabbit serum was used as a negative control. The cells were washed three times with PBS and incubated with a 1:500 dilution of Alexa Fluor 568-labeled secondary antibody for 60 min at room temperature. After being washed three times with PBS, the cells were incubated with 1 µg/ml 4′,6-diamidino-2-phenylindole (DAPI) for 5 min at room temperature and washed with PBS. The cells were mounted on a glass slide using a 9:1 mixture of glycerol and PBS and viewed using an LSM 510Meta confocal microscope (Carl Zeiss Inc., Oberkochen, Germany).

Uptake study of β-Ala-Lys-AMCA: The cells differentiated with FGF2 and 2% FBS were rinsed several times with PBS and incubated with DMEM/F12 containing 25 µM β-Ala-Lys-AMCA for 4 h at 37°C. After incubation, uptake of β-Ala-Lys-AMCA was stopped by washing with ice-cold PBS. The cells were fixed for 30 min at room temperature in 4% paraformaldehyde, and immunofluorescence staining was performed using the primary and secondary antibodies as described above. The cells were then mounted using a 9:1 mixture of glycerol and PBS and viewed using an LSM 510Meta confocal microscope.

Statistical analysis: Levels of statistical significance were assessed using Student's *t*-test, and multiple comparisons were performed using analysis of variance (ANOVA) followed by Tukey's test.

Results

Early stages of differentiation into intestinal cells: For efficient, selective, and direct differentiation, a protocol designed to mimic intestinal development is desirable. We attempted differentiation into enterocytes that mediate the formation of the definitive endoderm. Because the intestine is an endoderm-derived organ, the human iPS cells were initially differentiated into the endoderm using a high concentration of activin A (100 ng/ml). Subsequently, we investigated the effects of FGF2, FGF4, and Wnt3a, which promote the development of mid- and hindgut lineages,[24,25] during differentiation from the definitive endoderm to intestinal stem cells. In these experiments, mRNA expression of caudal type homeobox 2 (CDX2), a major transcription factor of intestinal development and cell differentiation,[26,27] was slightly
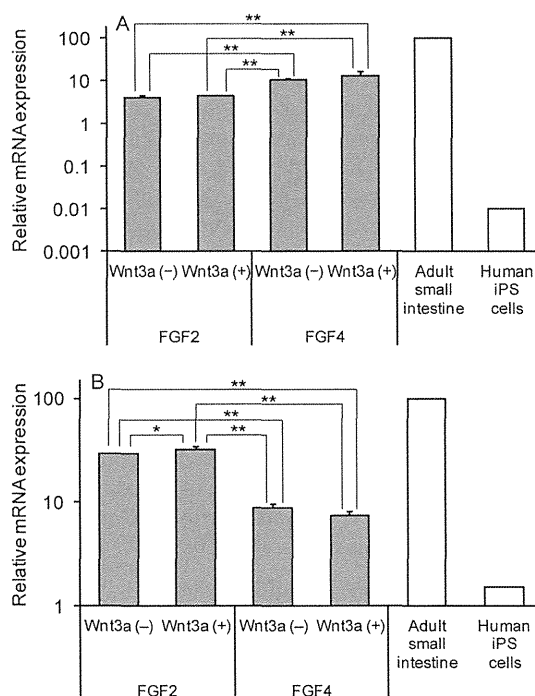

Fig. 2. Relative mRNA expression levels of CDX2 (A) and LGR5 (B) in differentiated intestinal stem cell-like cells
Human iPS cells were cultured in the presence of activin A for 3 days. The cells were further cultured in medium containing FGF2 or FGF4 with or without Wnt3a for 4 days and then in the presence of EGF for 1 day. After 8 days of differentiation, total RNA was extracted and mRNAs were analyzed by SYBR Green real-time RT-PCR. mRNA expression levels were normalized relative to that of GAPDH. Gene expression levels are represented relative to the level in the adult small intestine, which is set as 100. The adult small intestine and undifferentiated human iPS cells (shown as open columns) were used as positive and negative controls, respectively. Data are presented as the mean ± S.D. (*n* = 3), except for the adult small intestine and human iPS cells. Levels of statistical significance were compared among all groups: **p < 0.01, *p < 0.05.

higher in FGF4-treated cells than that in FGF2-treated cells (**Fig. 2A**). In contrast, mRNA expression of LGR5 in FGF4-treated cells was significantly lower than that in FGF2-treated cells (**Fig. 2B**). Under all conditions, these mRNA expression levels were higher than those in undifferentiated human iPS cells. No effects of Wnt3a were observed on mRNA expression of CDX2 or LGR5 during the early stages of differentiation.

Differentiation into enterocyte-like cells: To effectively differentiate human iPS cells into enterocyte-like cells, we examined

the effects of FBS concentration in the differentiation medium. Expression of LGR5 in differentiated human iPS cells did not differ in the presence of 2% or 10% FBS (**Fig. 3A**). However, mRNA expression of sucrase–isomaltase was 3.5-fold higher in 2% FBS than that in 10% FBS (**Fig. 3B**). In addition, mRNA expression levels of SLC15A1/peptide transporter 1 (PEPT1) and CYP3A4 were higher in the presence of 2% FBS (**Figs. 3C and 3D**). In differentiated enterocyte-like cells, sucrase–isomaltase and CYP3A4, which were not detected in undifferentiated human iPS cells, were expressed, and mRNA expression levels of LGR5 and SLC15A1/PEPT1 were 30–40-fold higher than those in undifferentiated human iPS cells. Morphological changes in differentiating human iPS cells are shown in **Figure 4**. Similar to ES cells, undifferentiated human iPS cells had little cytoplasm and were small in size (**Fig. 4A**). When human iPS cells were cultured in the presence of activin A and FGF2, the cells gradually exhibited morphological changes such as enlargement and acquisition of spiky shapes (**Fig. 4B**). At the final stage of differentiation with EGF and 2% FBS, a number of dome-like structures formed and were assumed to contain liquids and cells (**Figs. 4C and 4D**). In cells differentiated with activin A, FGF2, EGF, and 2% FBS, villin [28,29] and intestine specific homeobox (ISX)[30] were expressed, whereas intestinal fatty acid-binding protein (IFABP) was not expressed. Interestingly, mRNA expression levels of CDX2, dipeptidyl peptidase 4 (DPP4), and SLC46A1/proton-coupled folate transporter (PCFT) were similar to those in the adult small intestine, which was used as a positive control (**Fig. 5**). However, gene expression levels of UGT1A1 and ABCB1/multidrug resistance 1 (MDR1) were similar to those in undifferentiated human iPS cells (data not shown).

To determine the optimal duration of differentiation, we examined time-dependent variations in expression levels of specific small intestine genes such as LGR5, sucrase–isomaltase, and SLC15A1/PEPT1. After short-term culture (11 days), mRNA expression levels of sucrase–isomaltase and SLC15A1/PEPT1 were very low but gradually increased with differentiation until day 26. Similarly, CYP3A4 mRNA was not expressed after 11 days of differentiation but was expressed after 20 days (**Fig. 6**). LGR5 mRNA did not change with the duration of differentiation.

Immunofluorescence staining of sucrase–isomaltase in enterocyte-like cells: Sucrase–isomaltase is an essential carbohydrate digestion enzyme that is specifically expressed in brush border membranes of mature enterocytes. Therefore, sucrase–isomaltase expression is thought to be an indicator of differentiation into enterocytes. Indeed, protein expression of sucrase–isomaltase was confirmed in differentiated cells using immunofluorescence staining, in particular, in dense clusters of cells (**Fig. 7**).

Uptake of β-Ala-Lys-AMCA in enterocyte-like cells: Oligopeptide transporters are expressed in the brush border membrane and participate in peptide absorption from the intestinal lumen.[2] As shown in **Figure 3C**, expression of SLC15A1/PEPT1 mRNA in differentiated enterocyte-like cells was more than 30-fold higher than that in undifferentiated human iPS cells. To determine whether this leads to active peptide transport in differentiated cells, we performed peptide uptake assays using β-Ala-Lys-AMCA, a fluorescence-labeled substrate of the oligopeptide transporter.[31] As shown in **Figure 8**, intracellular uptake of β-Ala-Lys-AMCA was observed in cells expressing the sucrase–isomaltase proteins. However, uptake of β-Ala-Lys-AMCA at 4°C was low compared with that at 37°C (data not shown).
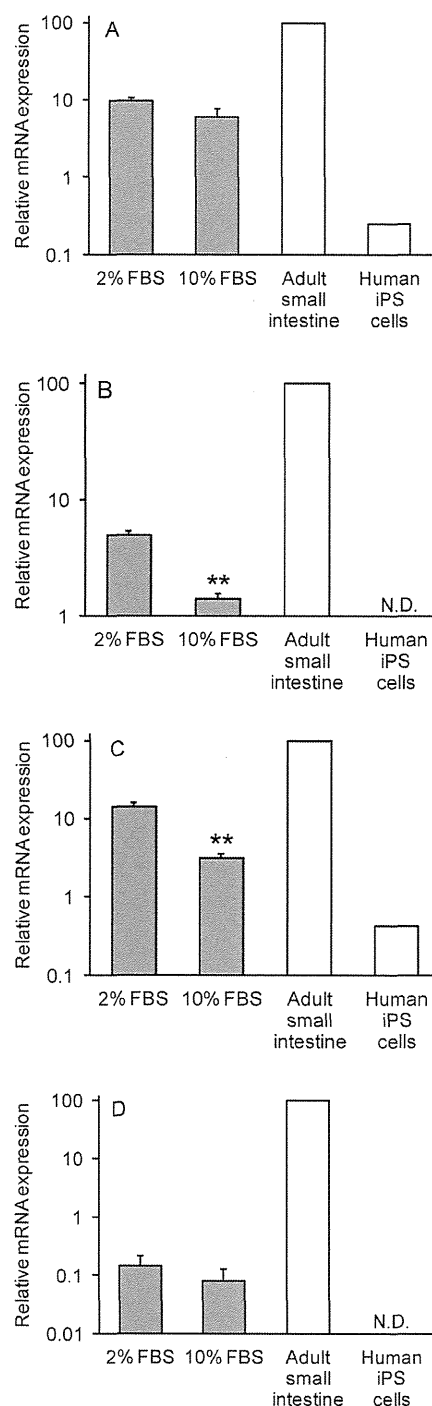

Fig. 3. Relative mRNA expression levels of LGR5 (A), sucrase–isomaltase (B), SLC15A1/PEPT1 (C), and CYP3A4 (D) in differentiated enterocyte-like cells cultured in 2% or 10% FBS
Human iPS cells were cultured in the presence of activin A for 3 days. The cells were further cultured in medium containing FGF2 for 4 days and then in the presence of 2% or 10% FBS and EGF for 17 days. After 24 days of differentiation, total RNA was extracted and mRNAs were analyzed by SYBR Green real-time RT-PCR. mRNA expression levels were normalized relative to that of GAPDH. Gene expression levels are represented relative to the level in the adult small intestine, which is set as 100. The adult small intestine and undifferentiated human iPS cells (shown as open columns) were used as positive and negative controls, respectively. Data are presented as the mean ± S.D. ($n = 3$), except for the adult small intestine and human iPS cells. N.D., not detected. Levels of statistical significance were compared with the 2% FBS group: **$p < 0.01$.
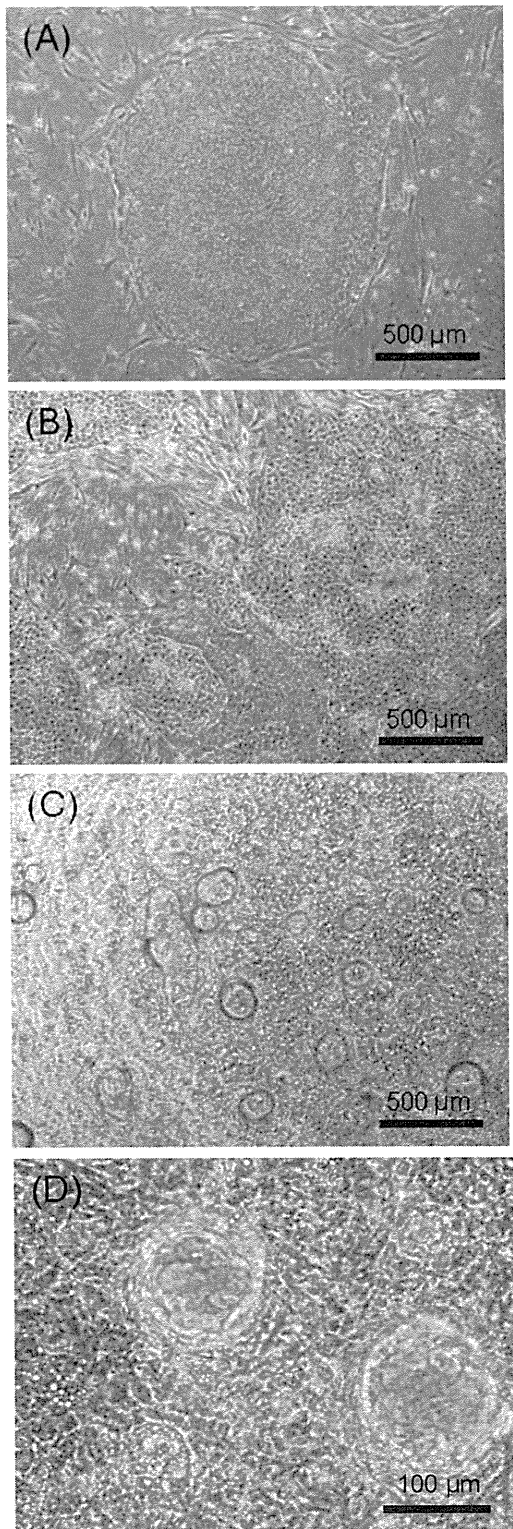
Fig. 4. Morphological changes in human iPS cells during differentiation into enterocyte-like cells

Human iPS cells were cultured in medium containing activin A for 3 days, FGF2 for 4 days, and 2% FBS and EGF for 17 days. (A) Undifferentiated human iPS cells; (B) midgut lineage cell-like cells after 7 days of differentiation; (C, D) enterocyte-like cells after 24 days of differentiation. Scale bar, 500 μm (A–C), 100 μm (D).
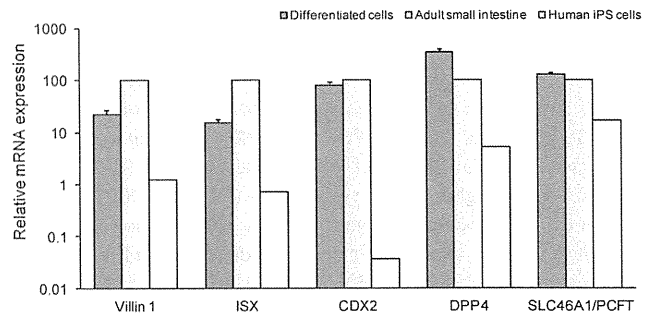

Fig. 5. Relative mRNA expression levels of the intestinal markers villin 1, ISX, CDX2, DPP4, and SLC46A1/PCFT in differentiated enterocyte-like cells

Human iPS cells were cultured in the presence of activin A for 3 days. The cells were further cultured in medium containing FGF2 for 4 days and then in the presence of 2% FBS and EGF for 19 days. After 26 days of differentiation, total RNA was extracted and mRNAs were analyzed by SYBR Green real-time RT-PCR. mRNA expression levels were normalized relative to that of GAPDH. Gene expression levels are represented relative to the level in the adult small intestine, which is set as 100. The adult small intestine and undifferentiated human iPS cells (shown as open columns) were used as positive and negative controls, respectively. Data are presented as the mean ± S.D. ($n = 3$), except for the adult small intestine and human iPS cells.
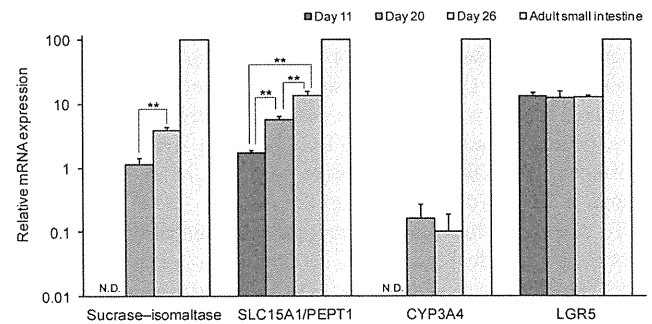

Fig. 6. Time-dependent variation in mRNA expression levels of sucrase–isomaltase, SLC15A1/PEPT1, CYP3A4, and LGR5 in differentiated entero-cyte-like cells

Human iPS cells were cultured in the presence of activin A for 3 days. The cells were further cultured in medium containing FGF2 for 4 days and then in the presence of 2% FBS and EGF for 4, 13, or 19 days. After 11, 20, or 26 days of differentiation, total RNA was extracted and mRNAs were analyzed by SYBR Green real-time RT-PCR. mRNA expression levels were normalized relative to that of GAPDH. Gene expression levels are represented relative to the level in the adult small intestine, which is set as 100. The adult small intestine was used as a positive control. Data are presented as the mean ± S.D. ($n = 4$) except for the adult small intestine. N.D., not detected. Levels of statistical significance were compared among all groups: **$p < 0.01$.

Discussion

Ueda et al.[14] reported the synthesis of gut-like organs from mouse iPS cells using the EB formulation technique with mouse ES cells. However, this hanging drop culture technique is hampered by its high requirement of skill, low EB formulation efficiency, unstable EB quality, and differing differentiation efficiencies between EBs. Spence et al.[15] reported the direct differentiation of human iPS cells into three-dimensional intestinal organoids. These organoids contained various cell types, including enterocytes, endocrine cells, goblet cells, and Paneth cells, although expression of drug-metabolizing enzymes and transporters, which are central to drug absorption and metabolism, was not examined. In their study, the intestinal crypt culture system, in which spheroids
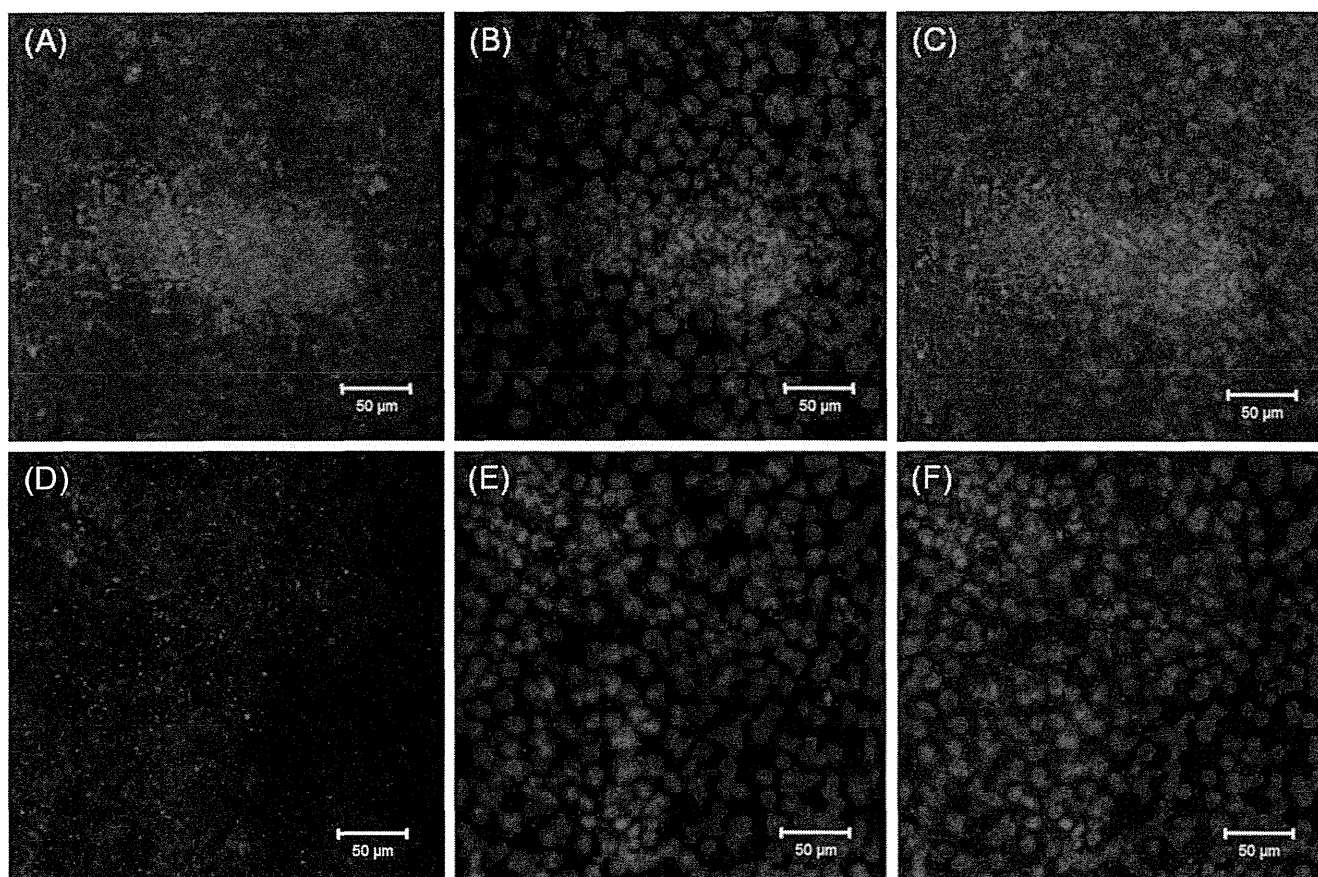
Fig. 7. Immunofluorescence analysis of sucrase–isomaltase in differentiated enterocyte-like cells
Human iPS cells were cultured in the presence of activin A for 3 days. The cells were further cultured in medium containing FGF2 for 4 days and then in the presence of 2% FBS and EGF for 19 days. After 26 days of differentiation, differentiated cells were stained with antisucrase–isomaltase antibody (A–C) or nonimmune rabbit serum as a negative control (D–F). Nuclei were counterstained with DAPI. (A) Immunofluorescence staining of sucrase–isomaltase (red); (D) immunofluorescence staining of rabbit serum as a negative control; (B, E) DAPI-stained DNA (blue); (C, F) overlay (Merge) image of sucrase–isomaltase and DAPI. Scale bar, 50 µm.
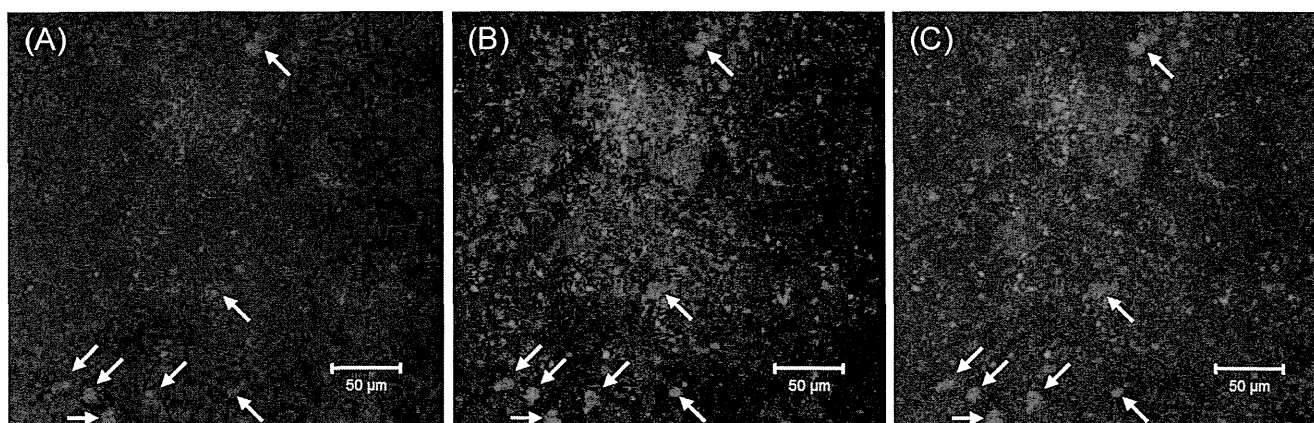
Fig. 8. Uptake of β-Ala-Lys-AMCA into differentiated enterocyte-like cells
Human iPS cells were cultured in the presence of activin A for 3 days. The cells were further cultured in medium containing FGF2 for 4 days and then in the presence of 2% FBS and EGF for 19 days. After 26 days of differentiation, the differentiated cells were incubated with β-Ala-Lys-AMCA (25 µM) for 4 h at 37°C. After uptake was stopped, the differentiated cells were fixed and stained with antisucrase–isomaltase antibody. Typical images from β-Ala-Lys-AMCA uptake experiments. Arrows indicate co-localization of β-Ala-Lys-AMCA and sucrase–isomaltase protein. (A) Intracellular uptake of β-Ala-Lys-AMCA (blue); (B) immunofluorescence staining of sucrase–isomaltase (red); (C) overlay (Merge) image of β-Ala-Lys-AMCA and sucrase–isomaltase. Scale bar, 50 µm.

are formed by three-dimensional culture, was applied during differentiation from the endoderm to intestinal organoids, and several factors were added in large quantities to induce differentiation. This method may be suitable for the culture of intestinal stem cells but not for selective differentiation into enterocytes, and it is complicated and costly. Therefore, we generated enterocyte-like cells using a simple two-dimensional culture method.

Spence *et al.*[15] also reported that the combination of FGF4 (500 ng/ml) and Wnt3a (500 ng/ml) effectively posteriorized the endoderm. Ameri *et al.*[32] reported the induction of CDX2 with FGF2 (256 ng/ml) in a concentration-dependent manner in the human ES cell-derived endoderm. In the present study, we examined the effects of FGF2, FGF4, and Wnt3a on the induction of the midgut endoderm lineage. Our results showed that the expression level of CDX2 was comparable in the FGF2 and FGF4 treatment groups, whereas no effect of Wnt3a was observed. These results were inconsistent with those of Spence *et al.*,[15] possibly because of the lower concentrations of Wnt3a used in our study (50 ng/ml). Sherwood *et al.*[33] demonstrated that β-catenin-dependent Wnt signaling, activated by the glycogen synthase kinase-3 (GSK3) inhibitor, induced the expression of the intestinal master regulator Cdx2 and induced intestinal differentiation of the ES cell-derived endoderm and large intestinal gene expression. They also indicated that because of poor bioactivity, the induction level of Cdx2 expression by Wnt3a was lower than that by the GSK3 inhibitor. Therefore, superior stability and bioactivity of small-molecule compounds may lead to more effective experimental regulation of these signaling pathways. However, the striking activation of Wnt signaling also induced large intestinal gene expression, and further investigations of the extent of activation of Wnt signaling during small intestinal differentiation may be required. The expression of LGR5[17] was higher in the FGF2 treatment group than that in the FGF4 treatment group. Therefore, subsequent differentiation experiments were performed using FGF2.

We have demonstrated that enterocyte-like cells, which express the specific intestinal markers sucrase–isomaltase,[34,35] villin 1, ISX, and pharmacokinetics-related genes, were differentiated from an intestinal stem cell-like cell population by two-dimensional culture with EGF and a low serum concentration. Sucrase–isomaltase and SLC15A1/PEPT1 mRNA gradually increased with the duration of differentiation, indicating that longer duration may be necessary to efficiently obtain mature enterocytes. In contrast, LGR5 mRNA expression remained unchanged, suggesting that enterocytes matured during intestinal stem cell proliferation. DPP4 (serine protease) and SLC46A1/PCFT (folate transporter) are known to be abundantly expressed in epithelial cells of the small intestine.[36,37] Expression of DPP4 and SLC46A1/PCFT in differentiated cells was higher than that in adult small intestine samples. Intestinal differentiation was promoted by low FBS concentrations in this study. Potentially, the growth of extra-enterocytic cells such as fibroblasts may be suppressed with decreasing FBS concentrations, and some differentiation and growth-inhibiting factors may be present in FBS, although the mechanisms underlying these effects remain unclear.

At present, human intestinal epithelial cells are difficult to obtain, and no appropriate model cell system exists. Instead, other tissue cell-derived cell lines, including Caco-2 cells (human colon carcinoma cell line) and Madin–Darby canine kidney (MDCK) cells, have been used as intestinal models in drug absorption studies.[2,38] However, drug transporter expression patterns in these

cells considerably differ from those in enterocytes. In particular, CYP3A4 is expressed at very low levels in these cell lines. In the present study, cells expressing the sucrase–isomaltase protein showed uptake of β-Ala-Lys-AMCA, the substrate of the oligopeptide transporter (**Fig. 8**). Differentiated cells also expressed CYP3A4 mRNA, albeit at levels lower than those in the adult small intestine (**Fig. 3**), suggesting that enterocyte-like cells differentiated from human iPS cells have peptide-transporting activity and may be useful in the study of drug absorbability.

In this study, we used a human iPS cell line, which is easily differentiated into hepatocytes of an endodermal lineage, because the intestine is also an endoderm-derived tissue. Differentiation propensity is known to be markedly different among human ES and iPS cell lines.[39,40] Thus, there may be a difference in the degree of intestinal differentiation depending on the human iPS cell line being tested. Regarding this point, we believe it is necessary to perform studies comparing intestinal differentiation among human iPS cell lines in the future.

In conclusion, because the intestine is an endoderm-derived tissue, human iPS cells were directly differentiated into the endoderm using activin A. Subsequently, we devised a simple method for differentiation into enterocyte-like cells with functional peptide transport by two-dimensional culture and the addition of several growth factors. These data suggest that human iPS-derived enterocytes may facilitate future drug development studies. If enterocyte-like cells, which have functional features similar to those of enterocytes, can be generated from human iPS cells, it may be possible to construct systems for easy estimation of overall intestinal function, including absorption and metabolism.

References

1) Paine, M. F., Hart, H. L., Ludington, S. S., Haining, R. L., Rettie, A. E. and Zeldin, D. C.: The human intestinal cytochrome P450 'pie'. *Drug Metab. Dispos.*, **34**: 880–886 (2006).
2) Giacomini, K. M., Huang, S.-M., Tweedie, D. J., Benet, L. Z., Brouwer, K. L. R., Chu, X., Dahlin, A., Evers, R., Fischer, V., *et al.*: Membrane transporters in drug development. *Nat. Rev. Drug Discov.*, **9**: 215–236 (2010).
3) Takahashi, K., Tanabe, K., Ohnuki, M., Narita, M., Ichisaka, T., Tomoda, K. and Yamanaka, S.: Induction of pluripotent stem cells from adult human fibroblasts by defined factors. *Cell*, **131**: 861–872 (2007).
4) Ochiya, T., Yamamoto, Y. and Banas, A.: Commitment of stem cells into functional hepatocytes. *Differentiation*, **79**: 65–73 (2010).
5) Tateishi, K., He, J., Taranova, O., Liang, G., D'Alessio, A. C. and Zhang, Y.: Generation of insulin-secreting islet-like clusters from human skin fibroblasts. *J. Biol. Chem.*, **283**: 31601–31607 (2008).
6) Zhang, D., Jiang, W., Liu, M., Sui, X., Yin, X., Chen, S., Shi, Y. and Deng, H.: Highly efficient differentiation of human ES cells and iPS cells into mature pancreatic insulin-producing cells. *Cell Res.*, **19**: 429–438 (2009).
7) Chambers, S. M., Fasano, C. A., Papapetrou, E. P., Tomishima, M., Sadelain, M. and Studer, L.: Highly efficient neural conversion of human ES and iPS cells by dual inhibition of SMAD signaling. *Nat. Biotechnol.*, **27**: 275–280 (2009).
8) Zhang, J., Wilson, G. F., Soerens, A. G., Koonce, C. H., Yu, J., Palecek, S. P., Thomson, J. A. and Kamp, T. J.: Functional cardiomyocytes derived from human induced pluripotent stem cells. *Circ. Res.*, **104**: e30–e41 (2009).
9) Song, Z., Cai, J., Liu, Y., Zhao, D., Yong, J., Duo, S., Song, X., Guo, Y., Zhao, Y., *et al.*: Efficient generation of hepatocyte-like cells from human induced pluripotent stem cells. *Cell Res.*, **19**: 1233–1242 (2009).
10) Sullivan, G. J., Hay, D. C., Park, I.-H., Fletcher, J., Hannoun, Z., Payne, C. M., Dalgetty, D., Black, J. R., Ross, J. A., *et al.*: Generation of functional human hepatic endoderm from human induced pluripotent stem cells. *Hepatology*, **51**: 329–335 (2010).
11) Si-Tayeb, K., Noto, F. K., Nagaoka, M., Li, J., Battle, M. A., Duris, C., North, P. E., Dalton, S. and Duncan, S. A.: Highly efficient generation of human hepatocyte-like cells from induced pluripotent stem cells.

Hepatology, **51**: 297–305 (2010).

12) Touboul, T., Hannan, N. R. F., Corbineau, S., Martinez, A., Martinet, C., Branchereau, S., Mainot, S., Strick-Marchand, H., Pedersen, R., *et al.*: Generation of functional hepatocytes from human embryonic stem cells under chemically defined conditions that recapitulate liver development. *Hepatology*, **51**: 1754–1765 (2010).

13) Takayama, K., Inamura, M., Kawabata, K., Tashiro, K., Katayama, K., Sakurai, F., Hayakawa, T., Furue, M. K. and Mizuguchi, H.: Efficient and directive generation of two distinct endoderm lineages from human ESCs and iPSCs by differentiation stage-specific SOX17 transduction. *PLoS ONE*, **6**: e21780 (2011).

14) Ueda, T., Yamada, T., Hokuto, D., Koyama, F., Kasuda, S., Kanehiro, H. and Nakajima, Y.: Generation of functional gut-like organ from mouse induced pluripotent stem cells. *Biochem. Biophys. Res. Commun.*, **391**: 38–42 (2010).

15) Spence, J. R., Mayhew, C. N., Rankin, S. A., Kuhar, M. F., Vallance, J. E., Tolle, K., Hoskins, E. E., Kalinichenko, V. V., Wells, S. I., *et al.*: Directed differentiation of human pluripotent stem cells into intestinal tissue in vitro. *Nature*, **470**: 105–109 (2011).

16) Scoville, D. H., Sato, T., He, X. C. and Li, L.: Current view: intestinal stem cells and signaling. *Gastroenterology*, **134**: 849–864 (2008).

17) Barker, N., van Es, J. H., Kuipers, J., Kujala, P., van den Born, M., Cozijnsen, M., Haegebarth, A., Korving, J., Begthel, H., *et al.*: Identification of stem cells in small intestine and colon by marker gene Lgr5. *Nature*, **449**: 1003–1007 (2007).

18) Sato, T., Vries, R. G., Snippert, H. J., van de Wetering, M., Barker, N., Stange, D. E., van Es, J. H., Abo, A., Kujala, P., *et al.*: Single Lgr5 stem cells build crypt-villus structures in vitro without a mesenchymal niche. *Nature*, **459**: 262–265 (2009).

19) Sato, T., Stange, D. E., Ferrante, M., Vries, R. G. J., van Es, J. H., van den Brink, S., van Houdt, W. J., Pronk, A., van Gorp, J., *et al.*: Long-term expansion of epithelial organoids from human colon, adenoma, adenocarcinoma, and Barrett's epithelium. *Gastroenterology*, **141**: 1762–1772 (2011).

20) D'Amour, K. A., Agulnick, A. D., Eliazer, S., Kelly, O. G., Kroon, E. and Baetge, E. E.: Efficient differentiation of human embryonic stem cells to definitive endoderm. *Nat. Biotechnol.*, **23**: 1534–1541 (2005).

21) McLean, A. B., D'Amour, K. A., Jones, K. L., Krishnamoorthy, M., Kulik, M. J., Reynolds, D. M., Sheppard, A. M., Liu, H., Xu, Y., *et al.*: Activin A efficiently specifies definitive endoderm from human embryonic stem cells only when phosphatidylinositol 3-kinase signaling is suppressed. *Stem Cells*, **25**: 29–38 (2007).

22) Ishizaki, T., Uehata, M., Tamechika, I., Keel, J., Nonomura, K., Maekawa, M. and Narumiya, S.: Pharmacological properties of Y-27632, a specific inhibitor of rho-associated kinases. *Mol. Pharmacol.*, **57**: 976–983 (2000).

23) Watanabe, K., Ueno, M., Kamiya, D., Nishiyama, A., Matsumura, M., Wataya, T., Takahashi, J. B., Nishikawa, S., Nishikawa, S., *et al.*: A ROCK inhibitor permits survival of dissociated human embryonic stem cells. *Nat. Biotechnol.*, **25**: 681–686 (2007).

24) Dessimoz, J., Opoka, R., Kordich, J. J., Grapin-Botton, A. and Wells, J. M.: FGF signaling is necessary for establishing gut tube domains along the anterior–posterior axis in vivo. *Mech. Dev.*, **123**: 42–55 (2006).

25) McLin, V. A., Rankin, S. A. and Zorn, A. M.: Repression of Wnt/β-catenin signaling in the anterior endoderm is essential for liver and pancreas development. *Development*, **134**: 2207–2217 (2007).

26) Escaffit, F., Paré, F., Gauthier, R., Rivard, N., Boudreau, F. and Beaulieu, J.-F.: Cdx2 modulates proliferation in normal human intestinal epithelial crypt cells. *Biochem. Biophys. Res. Commun.*, **342**: 66–72 (2006).

27) Gao, N., White, P. and Kaestner, K. H.: Establishment of intestinal identity and epithelial-mesenchymal signaling by Cdx2. *Dev. Cell*, **16**: 588–599 (2009).

28) Robine, S., Huet, C., Moll, R., Sahuquillo-Merino, C., Coudrier, E., Zweibaum, A. and Louvard, D.: Can villin be used to identify malignant and undifferentiated normal digestive epithelial cells? *Proc. Natl. Acad. Sci. USA*, **82**: 8488–8492 (1985).

29) Boller, K., Arpin, M., Pringault, E., Mangeat, P. and Reggio, H.: Differential distribution of villin and villin mRNA in mouse intestinal epithelial cells. *Differentiation*, **39**: 51–57 (1988).

30) Seino, Y., Miki, T., Kiyonari, H., Abe, T., Fujimoto, W., Kimura, K., Takeuchi, A., Takahashi, Y., Oiso, Y., *et al.*: Isx participates in the maintenance of vitamin A metabolism by regulation of beta-carotene 15,15'-monooxygenase (Bcmo1) expression. *J. Biol. Chem.*, **283**: 4905–4911 (2008).

31) Groneberg, D. A., Döring, F., Eynott, P. R., Fischer, A. and Daniel, H.: Intestinal peptide transport: ex vivo uptake studies and localization of peptide carrier PEPT1. *Am. J. Physiol. Gastrointest. Liver Physiol.*, **281**: G697–G704 (2001).

32) Ameri, J., Ståhlberg, A., Pedersen, J., Johansson, J. K., Johannesson, M. M., Artner, I. and Semb, H.: FGF2 specifies hESC-derived definitive endoderm into foregut/midgut cell lineages in a concentration-dependent manner. *Stem Cells*, **28**: 45–56 (2010).

33) Sherwood, R. I., Maehr, R., Mazzoni, E. O. and Melton, D. A.: Wnt signaling specifies and patterns intestinal endoderm. *Mech. Dev.*, **128**: 387–400 (2011).

34) Boudreau, F., Rings, E. H. H. M., van Wering, H. M., Kim, R. K., Swain, G. P., Krasinski, S. D., Moffett, J., Grand, R. J., Suh, E. R., *et al.*: Hepatocyte nuclear factor-1α, GATA-4, and caudal related homeodomain protein Cdx2 interact functionally to modulate intestinal gene transcription. *J. Biol. Chem.*, **277**: 31909–31917 (2002).

35) Gu, N., Adachi, T., Matsunaga, T., Tsujimoto, G., Ishihara, A., Yasuda, K. and Tsuda, K.: HNF-1α participates in glucose regulation of sucrase-isomaltase gene expression in epithelial intestinal cells. *Biochem. Biophys. Res. Commun.*, **353**: 617–622 (2007).

36) Qiu, A., Jansen, M., Sakaris, A., Min, S. H., Chattopadhyay, S., Tsai, E., Sandoval, C., Zhao, R., Akabas, M. H., *et al.*: Identification of an intestinal folate transporter and the molecular basis for hereditary folate malabsorption. *Cell*, **127**: 917–928 (2006).

37) Darmoul, D., Voisin, T., Couvineau, A., Rouyer-Fessard, C., Salomon, R., Wang, Y., Swallow, D. M. and Laburthe, M.: Regional expression of epithelial dipeptidyl peptidase IV in the human intestines. *Biochem. Biophys. Res. Commun.*, **203**: 1224–1229 (1994).

38) Volpe, D. A.: Drug-permeability and transporter assays in Caco-2 and MDCK cell lines. *Future Med. Chem.*, **3**: 2063–2077 (2011).

39) Osafune, K., Caron, L., Borowiak, M., Martinez, R. J., Fitz-Gerald, C. S., Sato, Y., Cowan, C. A., Chien, K. R. and Melton, D. A.: Marked differences in differentiation propensity among human embryonic stem cell lines. *Nat. Biotechnol.*, **26**: 313–315 (2008).

40) Kajiwara, M., Aoi, T., Okita, K., Takahashi, R., Inoue, H., Takayama, N., Endo, H., Eto, K., Toguchida, J., *et al.*: Donor-dependent variations in hepatic differentiation from human-induced pluripotent stem cells. *Proc. Natl. Acad. Sci. USA*, **109**: 12538–12543 (2012).

A calcium-dependent protease as a potential therapeutic target for Wolfram syndrome

Simin Lu[a,b], Kohsuke Kanekura[a], Takashi Hara[a], Jana Mahadevan[a], Larry D. Spears[a], Christine M. Oslowski[c], Rita Martinez[d], Mayu Yamazaki-Inoue[e], Masashi Toyoda[e], Amber Neilson[d], Patrick Blanner[d], Cris M. Brown[a], Clay F. Semenkovich[a], Bess A. Marshall[f], Tamara Hershey[g], Akihiro Umezawa[e], Peter A. Greer[h], and Fumihiko Urano[a,i,1]

[a]Department of Medicine, Division of Endocrinology, Metabolism, and Lipid Research, Washington University School of Medicine, St. Louis, MO 63110; [b]Graduate School of Biomedical Sciences, University of Massachusetts Medical School, Worcester, MA 01655; [c]Department of Medicine, Boston University School of Medicine, Boston, MA 02118; [d]Department of Genetics, iPSC core facility, Washington University School of Medicine, St. Louis, MO 63110; [e]Department of Reproductive Biology, National Center for Child Health and Development, Tokyo 157-8535, Japan; [f]Department of Pediatrics, Washington University School of Medicine, St. Louis, MO 63110; [g]Departments of Psychiatry, Neurology, and Radiology, Washington University School of Medicine, St. Louis, MO 63110; [h]Department of Pathology and Molecular Medicine, Queen's University, Division of Cancer Biology and Genetics, Queen's Cancer Research Institute, Kingston, Ontario K7L3N6, Canada; and [i]Department of Pathology and Immunology, Washington University School of Medicine, St. Louis, MO 63110

Wolfram syndrome is a genetic disorder characterized by diabetes and neurodegeneration and considered as an endoplasmic reticulum (ER) disease. Despite the underlying importance of ER dysfunction in Wolfram syndrome and the identification of two causative genes, Wolfram syndrome 1 (*WFS1*) and Wolfram syndrome 2 (*WFS2*), a molecular mechanism linking the ER to death of neurons and β cells has not been elucidated. Here we implicate calpain 2 in the mechanism of cell death in Wolfram syndrome. Calpain 2 is negatively regulated by WFS2, and elevated activation of calpain 2 by WFS2-knockdown correlates with cell death. Calpain activation is also induced by high cytosolic calcium mediated by the loss of function of WFS1. Calpain hyperactivation is observed in the WFS1 knockout mouse as well as in neural progenitor cells derived from induced pluripotent stem (iPS) cells of Wolfram syndrome patients. A small-scale small-molecule screen targeting ER calcium homeostasis reveals that dantrolene can prevent cell death in neural progenitor cells derived from Wolfram syndrome iPS cells. Our results demonstrate that calpain and the pathway leading its activation provides potential therapeutic targets for Wolfram syndrome and other ER diseases.

Wolfram syndrome | endoplasmic reticulum | diabetes | neurodegeneration | treatment

The endoplasmic reticulum (ER) takes center stage for protein production, redox regulation, calcium homeostasis, and cell death (1, 2). It follows that genetic or acquired ER dysfunction can trigger a variety of common diseases, including neurodegenerative diseases, metabolic disorders, and inflammatory bowel disease (3, 4). Breakdown in ER function is also associated with genetic disorders such as Wolfram syndrome (5–8). It is challenging to determine the exact effects of ER dysfunction on the fate of affected cells in common diseases with polygenic and multifactorial etiologies. In contrast, we reasoned that it should be possible to define the role of ER dysfunction in mechanistically homogenous patient populations, especially in rare diseases with a monogenic basis, such as Wolfram syndrome (9).

Wolfram syndrome (OMIM 222300) is a rare autosomal recessive disorder characterized by juvenile-onset diabetes mellitus and bilateral optic atrophy (7). Insulin-dependent diabetes usually occurs as the initial manifestation during the first decade of life, whereas the diagnosis of Wolfram syndrome is invariably later, with onset of symptoms in the second and ensuing decades (7, 10, 11). Two causative genes for this genetic disorder have been identified and named Wolfram syndrome 1 (*WFS1*) and Wolfram syndrome 2 (*WFS2*) (12, 13). It has been shown that multiple mutations in the *WFS1* gene, as well as a specific mutation in the *WFS2* gene, lead to β cell death and neurodegeneration through ER and mitochondrial dysfunction (5, 6, 14–16). *WFS1*

gene variants are also associated with a risk of type 2 diabetes (17). Moreover, a specific *WFS1* variant can cause autosomal dominant diabetes (18), raising the possibility that this rare disorder is relevant to common molecular mechanisms altered in diabetes and other human chronic diseases in which ER dysfunction is involved.

Despite the underlying importance of ER malfunction in Wolfram syndrome, and the identification of *WFS1* and *WFS2* genes, a molecular mechanism linking the ER to death of neurons and β cells has not been elucidated. Here we show that the calpain protease provides a mechanistic link between the ER and death of neurons and β cells in Wolfram syndrome.

Results

The causative genes for Wolfram syndrome, *WFS1* and *WFS2*, encode transmembrane proteins localized to the ER (5, 12, 13). Mutations in the *WFS1* or *WFS2* have been shown to induce neuronal and β cell death. To determine the cell death pathways emanating from the ER, we sought proteins associated with Wolfram syndrome causative gene products. HEK293 cells were transfected with a GST-tagged WFS2 expression plasmid. The GST-WFS2 protein was purified along with associated proteins on a glutathione affinity resin. These proteins were separated by

Significance

Wolfram syndrome is an autosomal recessive disorder characterized by juvenile diabetes and neurodegeneration, and is considered a prototype of human endoplasmic reticulum (ER) disease. Wolfram syndrome is caused by loss of function mutations of Wolfram syndrome 1 or Wolfram syndrome 2 genes, which encode transmembrane proteins localized to the ER. Despite its rarity, Wolfram syndrome represents the best human disease model currently available to identify drugs and biomarkers associated with ER health. Furthermore, this syndrome is ideal for studying the mechanisms of ER stress-mediated death of neurons and β cells. Here we report that the pathway leading to calpain activation offers potential drug targets for Wolfram syndrome and substrates for calpain might serve as biomarkers for this syndrome.

SDS/PAGE and visualized by Coomassie staining. Matrix-assisted laser desorption/ionization-time of flight (MALDI-TOF) mass spectroscopic analysis revealed 13 interacting proteins (Table S1), and one of the WFS2-associated polypeptides was CAPN2, the catalytic subunit of calpain 2, a member of the calcium dependent cysteine proteases family whose members mediate diverse biological functions including cell death (19–21) (Fig. 1A). Previous studies have shown that calpain 2 activation is regulated on the ER membrane and it plays a role in ER stress-induced apoptosis and β cell death (20, 22–24), which prompted us to study the role of WFS2 in calpain 2 activation.

Calpain 2 is a heterodimer consisting the CAPN2 catalytic subunit and the CAPNS1 (previously known as CAPN4) regulatory subunit. We first verified that WFS2 interacts with calpain 2 by showing that endogenous calpain 2 subunits CAPN2 (Fig. 1B) and CAPNS1 (Fig. 1C) each associated with GST-tagged WFS2 expressed in HEK293 cells. Endogenous CAPN2 was also found to be coimmunoprecipated with N- or C-terminal FLAG-tagged WFS2 expressed in HEK293 cells (Fig. S1A and B, respectively). To further confirm these findings, we performed a coimmunoprecipitation experiment in Neuro2a cells (a mouse neuroblastoma cell line) and INS-1 832/13 cells (a rat pancreatic β cell line)
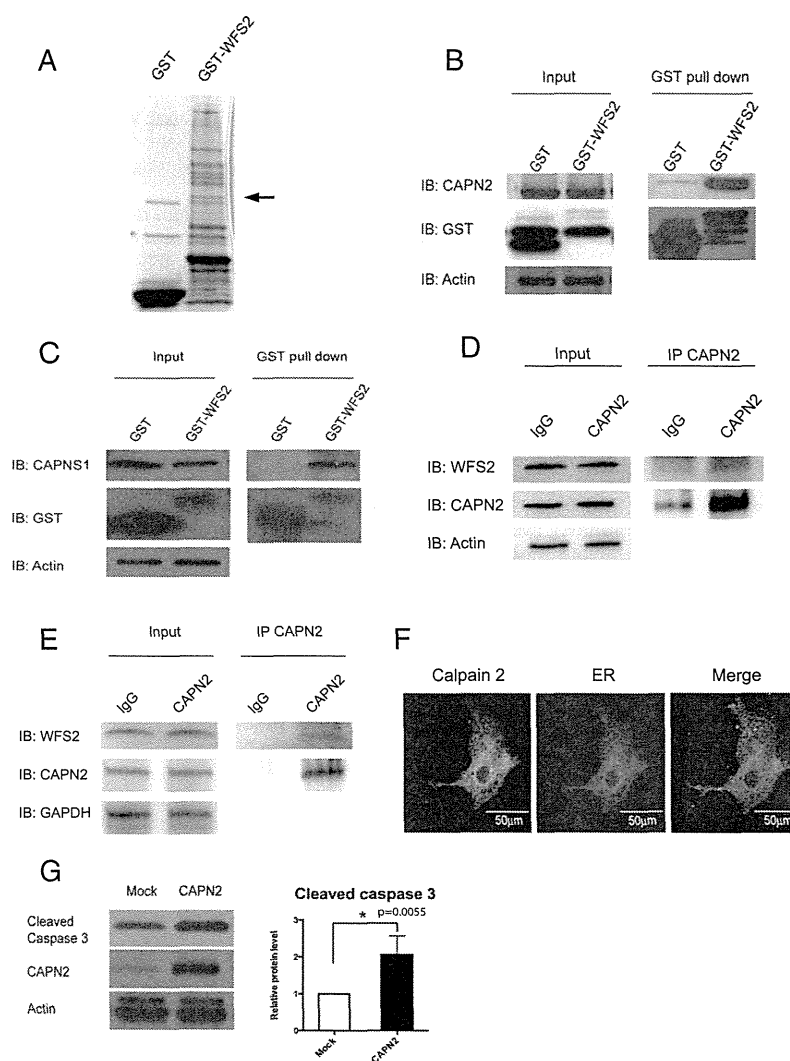
Fig. 1.   WFS2 interacts with CAPN2. (A) Affinity purification of WFS2-associated proteins from HEK293 cells transfected with GST or GST-WFS2 expression plasmid. Proteins were separated by SDS/PAGE and visualized by Coomassie blue staining. CAPN2 was identified by MALDI-TOF analysis and denoted by an arrow. (B) GST-tagged WFS2 was pulled down on a glutathione affinity resin from lysates of HEK293 cells transfected with a GST-WFS2 expression plasmid, and the pulled-down products were analyzed for CAPN2 by immunoblotting with anti-CAPN2 antibody. (C) GST-tagged WFS2 was pulled down on a glutathione affinity resin from lysates of HEK293 cells transfected with GST-WFS2 expression plasmid and the pulled-down products were analyzed for CAPNS1 by immunoblotting with anti-CAPNS1 antibody. (D) Lysates of Neuro2a cells were immunoprecipitated with IgG or anti-calpain 2 antibodies. Lysates of IgG and anti-calpain 2 immunoprecipitates were analyzed for WFS2, CAPN2 or actin by immunoblotting. (E) Lysates of INS-1 832/13 cells were immunoprecipitated with IgG or anti-calpain 2 antibody. Lysates of IgG and anti-calpain 2 immunoprecipitates were analyzed for WFS2, CAPN2 or actin by immunoblotting. (F) COS7 cells were transfected with pDsRed2-ER vector (Center) and stained with anti-calpain 2 antibody (Left). (Right) A merged image is shown. (G) HEK293 cells were transfected with empty expression plasmid or a CAPN2 expression plasmid. Apoptosis was monitored by immunoblotting analysis of caspase 3 cleavage. (Left) Expression levels of CAPN2 and actin were measured by immunoblotting. (Right) Quantification of immunoblot is shown (n = 3, *P < 0.05).

and found that endogenous WFS2 interacted with endogenous CAPN2 (Fig. 1 *D* and *E*). WFS2 is known to be a transmembrane protein localized to the ER. We therefore explored the possibility that calpain 2 might also localize to the ER. We transfected COS7 cells with pDsRed2-ER vector to visualize ER. Immunofluorescence staining of COS7 cells showed that endogenous calpain 2 was mainly localized to the cytosol, but also showed that a small portion colocalized with DsRed2-ER protein at the ER (Fig. 1*F*). Cell fractionation followed by immunoblot further confirmed this observation (Fig. S1*C*). Collectively, these results suggest that calpain 2 interacts with WFS2 at the cytosolic face of the ER.

Calpain hyperactivation has been shown to contribute to cell loss in various diseases (19), raising the possibility that calpain 2 might be involved in the regulation of cell death. To verify this issue, we overexpressed CAPN2, the catalytic subunit of calpain 2, and observed increase of cleaved caspase-3 in HEK293 cells indicating that hyperactivation of calpain 2 induces cell death (Fig. 1*G*).

To determine whether WFS2 plays a role in cell survival, we suppressed WFS2 expression in mouse neuronal NSC34 cells using siRNA and measured cell death under normal and ER stress conditions. WFS2 knockdown was associated with increased cleavage of caspase-3 in normal or ER stressed conditions (Fig. 2*A* and *B*). We subsequently evaluated calpain 2 activation by measuring the cleavage of alpha II spectrin, a substrate for calpain 2. RNAi-mediated knockdown of WFS2 induced calpain activation, especially under ER stress conditions (Fig. 2*A*).

In patients with Wolfram syndrome, destruction of β cells leads to juvenile-onset diabetes (25). This finding prompted us to examine whether WFS2 was also involved in pancreatic β cell death. As was seen in neuronal cells, knockdown of WFS2 in rodent β cell lines INS1 832/13 (Fig. 2*C*) and MIN6 (Fig. S2) was also associated with increased caspase-3 cleavage under both normal and ER stress conditions. The association of WFS2 with calpain 2 and their involvement in cell viability suggested that calpain 2 activation might be the cause of cell death in WFS2-deficient cells. To further explore the relationship between WFS2 and calpain 2, we expressed WFS2 together with the calpain 2 catalytic subunit CAPN2 and measured apoptosis. Ectopic expression of WFS2 significantly suppressed calpain 2-associated apoptosis under normal and ER stress conditions (Fig. 2*D*, lane 4 and lane 8, and Fig. 2*E*). Next, we tested whether CAPN2 mediates cell death induced by WFS2 deficiency. When CAPN2 was silenced in WFS2-deficient cells, apoptosis was partially suppressed compared with untreated WFS2-deficient cells (Fig. 2*F*). Taken together, these results suggest that WFS2 is a negative regulator of calpain 2 proapoptotic functions.

To further confirm that loss of function of WFS2 leads to cell death mediated by calpain 2, we tested if calpeptin, a calpain inhibitor, could prevent cell death in WFS2-deficient cells. In agreement with previous observations, calpeptin treatment prevented WFS2-knockdown-mediated cell death in neuronal (Fig. 3*A* and *B*) and β cell lines (Fig. 3*C* and Fig. S3*A*). Collectively, these results indicate that WFS2 is a suppressor of calpain 2-mediated cell death.

CAPN2 is the catalytic subunit of calpain 2. CAPN2 forms a heterodimer with the regulatory subunit, CAPNS1, which is required for protease activity and stability. We next explored the role of WFS2 in CAPN2 and CAPNS1 protein stability. Ectopic expression or RNAi-mediated knockdown of WFS2 did not correlate with changes in the steady-state expression of CAPN2 (Fig. S3*B*). By contrast, overexpression of WFS2 significantly reduced CAPNS1 protein expression (Fig. 3*D*) and transient suppression of WFS2 slightly increased CAPNS1 protein expression (Fig. 3*D*). These data suggest that WFS2 might be involved in CAPNS1 protein turnover, which is supported by the data showing that GST-tagged WFS2 expressed in HEK293 cells associated with endogenous CAPNS1 (Fig. 1*C*). To investigate whether WFS2 regulates CAPNS1 stability through the ubiquitin-proteasome pathway, we treated HEK293 cells ectopically

expressing WFS2 with a proteasome inhibitor, MG132, and then measured CAPNS1 protein level. MG132 treatment stabilized CAPNS1 protein in cells ectopically expressing WFS2 (Fig. 3*E*). Furthermore, we performed cycloheximide chase experiments using HEK293 cells ectopically expressing WFS2 and quantified CAPNS1 protein levels at different time points. Ectopic expression of WFS2 was associated with significantly accelerated CAPNS1 protein loss, indicating that WFS2 contributes to posttranslational regulation of CAPNS1 (Fig. 3*F*). To further assess whether WFS2 is involved in the ubiquitination of CAPNS1, we measured the levels of CAPNS1 ubiquitination in cells ectopically expressing WFS2 and observed that CAPNS1 ubiquitination was increased by ectopic expression of WFS2 (Fig. 3*G*).

To further investigate the role of WFS2 in calpain 2 regulation, we collected brain lysates from WFS2 knockout mice. Measured levels of cleaved spectrin, a well characterized substrate for calpain (26). Notably, protein expression levels of cleaved spectrin, as well as CAPNS1, were significantly increased in WFS2 knockout mice compared with control mice (Fig. 3*H*). Collectively, these results indicate that WFS2 inhibits calpain 2 activation by regulating CAPNS1 degradation mediated by the ubiquitin-proteasome system.

Calpain 2 is a calcium-dependent protease. *WFS1*, the other causative gene for Wolfram syndrome, has been shown to be involved in calcium homeostasis (27, 28), suggesting that the loss of function of WFS1 may also cause calpain activation. To evaluate this possibility, we measured calpain activation levels in brain tissues from WFS1 brain-specific knockout and control mice. We observed a significant increase in a calpain-specific spectrin cleavage product, reflecting higher calpain activation levels in WFS1 knockout mice compared with control mice (Fig. 4*A*). The suppression levels of WFS1 in different parts of the brain were shown in Fig. 4*B*. To further confirm that calpain is activated by the loss of WFS1, we looked for other calpain substrates in brain tissues from WFS1 knockout mice using a proteomics approach. Two-dimensional fluorescence gel electrophoresis identified 12 proteins differentially expressed between cerebellums of WFS1 knockout mice and those of control mice (Fig. 4 *C* and *D*). Among these, myelin basic protein (MBP) is a known substrate for calpain in the brain (29). We measured myelin basic protein levels in brain lysates from WFS1 knockout and control mice. Indeed, the cleavage and degradation of myelin basic protein was increased in WFS1 knockout mice relative to control mice (Fig. 4*E*).

Next, we looked for evidence of increased calpain activity in Wolfram syndrome patient cells. We created neural progenitor cells derived from induced pluripotent stem cells (iPSCs) of Wolfram syndrome patients with mutations in *WFS1*. Fibroblasts from four unaffected controls and five patients with Wolfram syndrome were transduced with four reprogramming genes (Sox2, Oct4, c-Myc, and Klf4) (30) (Table S2). We produced at least 10 iPSC clones from each control and Wolfram patient. All control- and Wolfram-iPSCs, exhibited characteristic human embryonic stem cell morphology, expressed pluripotency markers including ALP, NANOG, SOX2, SSEA4, TRA-1–81, and had a normal karyotype (Fig. 5 *A–F*). To create neural progenitor cells, we first formed neural aggregates from iPSCs. Neural aggregates were harvested at day 5, replated onto new plates to give rise to colonies containing neural rosette structures. At day 12, neural rosette clusters were collected, replated, and used as neural progenitor cells. Consistent with the data from WFS1 and WFS2 knockout mice, we observed that spectrin cleavage was increased in neural progenitor cells derived from Wolfram-iPSCs relative to control iPSCs, which indicates increased calpain activity (Fig. 5*G*).

Because calpain is known to be activated by high calcium, we explored the possibility that cytoplasmic calcium may be increased in patient cells by staining neural progenitor cells derived from
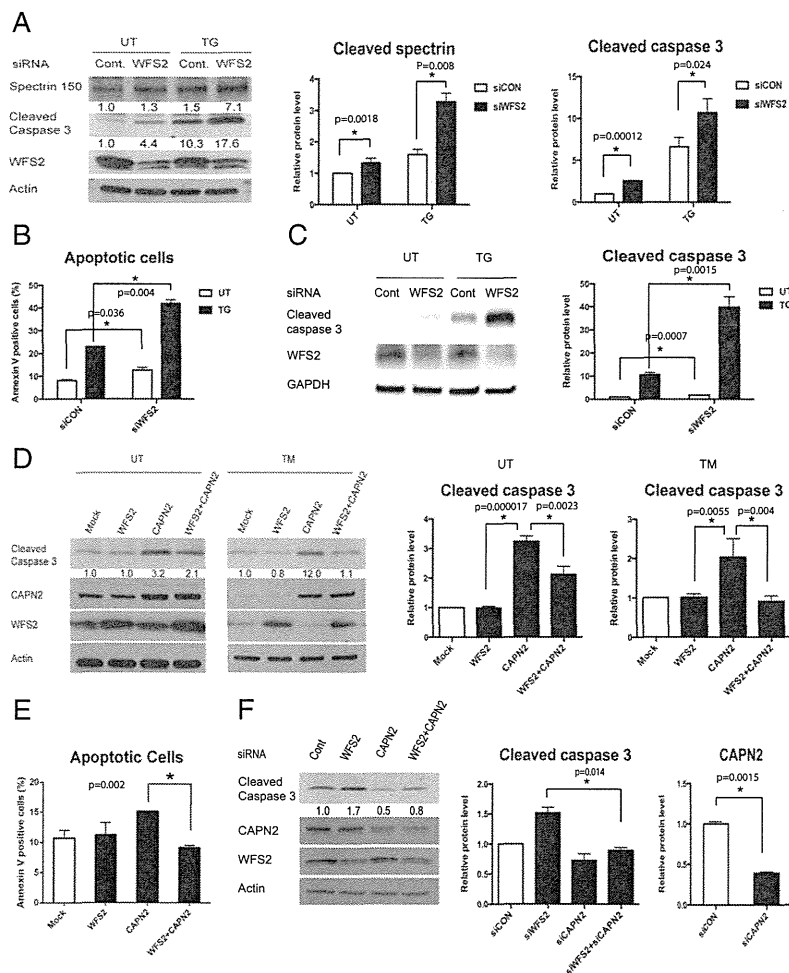
Fig. 2. WFS2 suppresses cell death mediated by CAPN2. (*A*) NSC34 cells were transfected with control scrambled siRNA or siRNA directed against WFS2, and then treated with 0.5µM thapsigargin (TG) for 6 h or untreated (UT). Apoptosis was monitored by immunoblotting analysis of cleaved caspase 3. (*Left*) Protein levels of cleaved spectrin, WFS2, and actin were measured by immunoblotting. (*Right*) Quantifications of cleaved spectrin and cleaved caspase 3 are shown ($n = 5$, *$P < 0.05$). (*B*) NSC34 cells were transfected with control scrambled siRNA or siRNA directed against WFS2, and then treated with 0.5 µM thapsigargin (TG) for 6 h or untreated (UT). Apoptosis was monitored by Annexin V staining followed by flow cytometry analysis. ($n = 3$, *$P < 0.05$). (*C*) INS-1 832/13 cells were transfected with control scrambled siRNA or siRNA directed against WFS2, and then treated with 0.5 µM thapsigargin (TG) for 6 h or untreated (UT). (*Left*) Expression levels of cleaved caspase 3, WFS2, and actin were measured by immunoblotting. (*Right*) Protein levels of cleaved caspase 3 are quantified ($n = 3$, *$P < 0.05$). (*D*) NSC34 cells were transfected with empty expression plasmid (Mock), WFS2 expression plasmid, CAPN2 expression plasmid or cotransfected with WFS1 and CAPN2 expression plasmids. Twenty-four h post transfection, cells were treated with 5 µg/mL tunicamycin (TM) for 16 h or untreated (UT). Apoptosis was monitored by immunoblotting analysis of the relative levels of cleaved caspase 3 (indicated in *Left*). Expression levels of CAPN2, WFS2, and actin were also measured by immunoblotting. Quantification of cleaved caspase 3 levels under untreated (*Center*) and tunicamycin treated (*Right*) conditions are shown as bar graphs. ($n = 5$, *$P < 0.05$). (*E*) Neuro2a cells transfected with empty expression plasmid (Mock), WFS2 expression plasmid, CAPN2 expression plasmid or cotransfected with WFS1 and CAPN2 expression plasmids were examined for apoptosis by Annexin V staining followed by flow cytometry analysis (*Right*, $n = 3$, *$P < 0.05$). (*F*) NSC34 cells were transfected with scrambled siRNA (Cont), WFS2 siRNA, CAPN2 siRNA or cotransfected with WFS2 siRNA and CAPN2 siRNA. Apoptosis was detected by immunoblotting of cleaved caspase 3. (*Left*) Protein levels of CAPN2, WFS2 and actin were also shown. (*Right*) Quantification of immunoblotting is shown ($n = 3$, *$P < 0.05$).

control- and Wolfram-iPSCs with Fura-2, a fluorescent calcium indicator which enables accurate measurements of cytoplasmic calcium concentrations. Fig. 5*H*, *Left*, shows that cytoplasmic calcium levels were higher in Wolfram-iPSC-derived neuronal cells relative to control cells. This result was confirmed by staining these cells with another fluorescent calcium indicator, Fluo-4 (Fig. 5*H*, *Right*). Collectively, these results indicate that loss of function of WFS1 increases cytoplasmic calcium levels, leading to calpain activation.

The results shown above argue that the pathway leading to calpain activation provides potential therapeutic targets for Wolfram syndrome. To test this concept, we elected to focus on modulating cytosolic calcium and performed a small-scale screen to identify chemical compounds that could prevent cell death mediated by thapsigargin, a known inhibitor for ER calcium ATPase. Among 73 well characterized chemical compounds that we tested (Table S3), 8 could significantly suppress thapsigargin-mediated cell death. These were PARP inhibitor, dantrolene, NS398, pioglitazone, calpain inhibitor III, docosahexaenoic acid (DHA), rapamycin, and GLP-1 (Fig. 6*A*). GLP-1, pioglitazone, and rapamycin are FDA-approved drugs and have been shown to confer protection against ER stress-mediated cell death (27, 31–33). Dantrolene is another FDA-approved drug clinically used for muscle spasticity and malignant hyperthermia (34). Previous studies
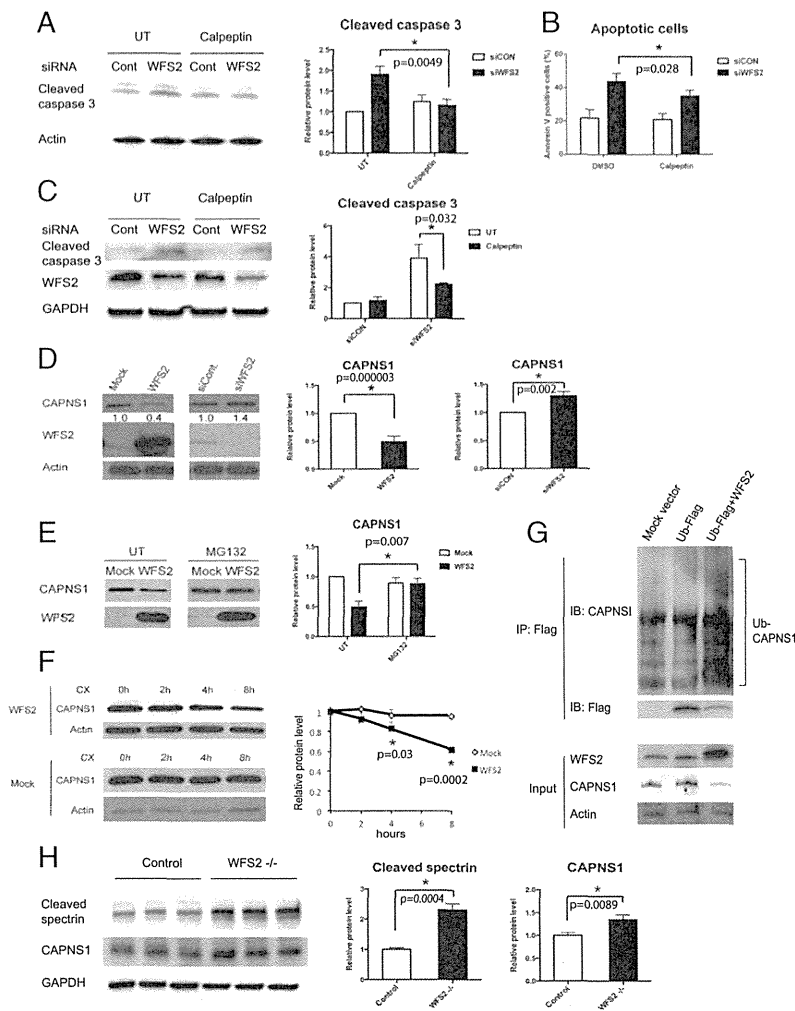
Fig. 3. WFS2 regulates calpain activity through CAPNS1. (A) Neuro-2a cells were transfected with siRNA against WFS2 or a control scrambled siRNA. Thirty-six h after transfection, cells were treated with or without 100μM calpeptin for 12 h. Cleaved caspase 3 and actin levels were assessed by immunoblotting (left panel). Cleaved caspase 3 protein levels are quantified in the right panel ($n = 3$, $*P < 0.05$). (B) Neuro-2a cells were transfected with siRNA against WFS2 or scrambled siRNA. Thirty-six h after transfection, cells were treated with or without 100 μM calpeptin for 12 h. Early stage apoptosis was monitored by Annexin V staining followed by flow cytometry ($n = 3$, $*P < 0.05$). (C) INS-1 832/13 cells were transfected with scrambled siRNA and WFS2 siRNA. Twenty-four h after transfection, cells were treated with or without 5 μM calpeptin for 24 h. Cleaved caspase 3, WFS2 and actin levels were monitored by immunoblotting (Left) and quantified (Right) ($n = 3$, $*P < 0.05$). (D, Left) CAPNS1, WFS2, and actin levels were assessed by immunoblotting in HEK293 cells transfected with empty expression plasmid (Mock), WFS2 expression plasmid, scrambled siRNA (siCON), or WFS2 siRNA (siWFS2). (D, Right) Protein levels of CAPNS1 are quantified ($n = 5$, $*P < 0.05$). (E) HEK293 cells were transfected with empty (Mock) or WFS2 expression plasmid, and then treated with MG132 (2 μM) or untreated (UT). Expression levels of CAPNS1 and WFS2 were measured by immunoblotting (Left) and quantified (Right) ($n = 4$, $*P < 0.05$). (F) HEK293 cells were transfected with empty or WFS2 expression plasmid, and then treated with cycloheximide (100 μM) for indicated times. (Left) Expression levels of CAPNS1 and actin were measured by immunoblotting. (Right) Band intensities corresponding to CAPNS1 in Left were quantified by Image J and plotted as relative rates of the signals at 0 h ($n = 3$, $*P < 0.05$). (G) NSC34 cells were transfected with mock empty vector, FLAG tagged ubiquitin (Ub-FLAG) plasmid or cotransfected with WFS2 expression plasmid and Ub-FLAG plasmid. Cell lysates were immunoprecipitated with FLAG affinity beads and analyzed for ubiquitin conjugated proteins by immunoblotting. Levels of CAPNS1 and Ub-FLAG protein were measured in the precipitates. WFS2, CAPNS1 and actin expression was monitored in the input samples. (H) Brain lysates from control and WFS2 knockout mice were analyzed by immunoblotting. Protein levels of cleaved spectrin and CAPNS1 were determined (Left) and quantified (Center and Right) (each group $n = 3$, $*P < 0.05$).

have shown that dantrolene is an inhibitor of the ER-localized ryanodine receptors and suppresses leakage of calcium from the ER to cytosol (35, 36). We thus hypothesized that dantrolene could confer protection against cell death in Wolfram syndrome, and performed a series of experiments to investigate this possibility. We first examined whether dantrolene could decrease cytoplasmic calcium levels. As expected, dantrolene treatment decreased cytosolic calcium levels in INS-1 832/13 and NSC34 cells (Fig. S4 A and B). We next asked whether dantrolene could

restore cytosolic calcium levels in WFS1-deficient cells. RNAi-mediated WFS1 knockdown increased cytosolic calcium levels relative to control cells, and dantrolene treatment restored cytosolic calcium levels in WFS1-knockdown INS-1 832/13 cells (Fig. 6B, Left) as well as WFS1-knockdown NSC34 cells (Fig. 6B, Right). Next, to determine whether dantrolene confered protection in WFS1-deficient cells, we treated WFS1 silenced INS-1 832/13 cells with dantrolene and observed suppression of apoptosis (Fig. 6C) and calpain activity (Fig. 6D). Dantrolene treatment also prevented
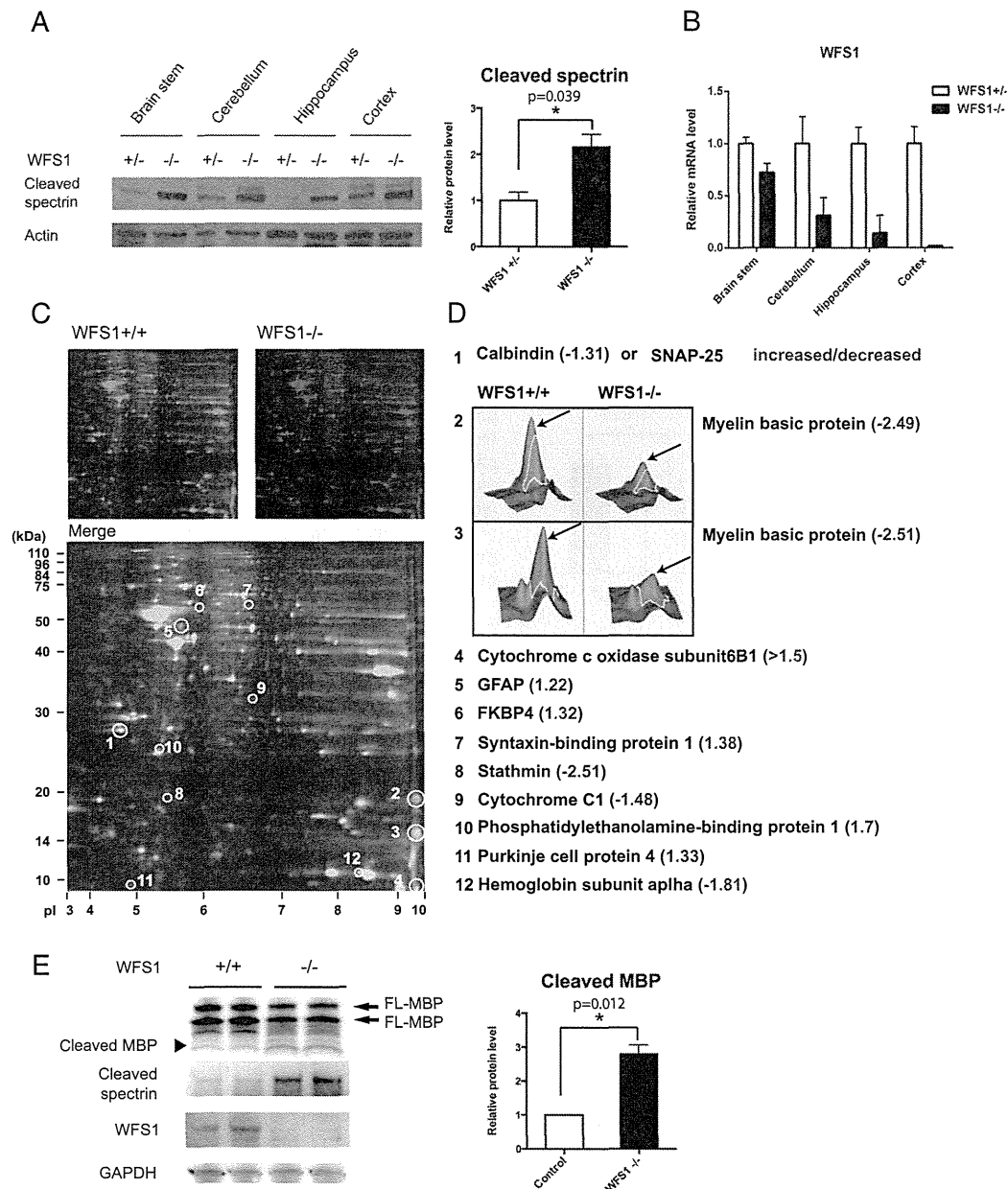
A

WFS1

Cleaved spectrin

Actin

Cleaved spectrin
p=0.039

B

WFS1

☐ WFS1+/-
■ WFS1-/-

C

WFS1+/+   WFS1-/-

Merge

(kDa)
110
96
84
75
50
40
30
20
14
10

pI 3 4 5 6 7 8 9 10

D

1 Calbindin (-1.31) or SNAP-25 increased/decreased

WFS1+/+   WFS1-/-

2 Myelin basic protein (-2.49)

3 Myelin basic protein (-2.51)

4 Cytochrome c oxidase subunit6B1 (>1.5)
5 GFAP (1.22)
6 FKBP4 (1.32)
7 Syntaxin-binding protein 1 (1.38)
8 Stathmin (-2.51)
9 Cytochrome C1 (-1.48)
10 Phosphatidylethanolamine-binding protein 1 (1.7)
11 Purkinje cell protein 4 (1.33)
12 Hemoglobin subunit aplha (-1.81)

E

WFS1   +/+   -/-

← FL-MBP
← FL-MBP

Cleaved MBP ▶

Cleaved spectrin

WFS1

GAPDH

Cleaved MBP
p=0.012

Fig. 4. Evidence of Calpain 2 activation in a mouse model of Wolfram syndrome. (*A*) Protein was extracted from brain tissues of WFS1 brain-specific knockout (−/−) and control (+/−) mice. (*Left*) Cleaved alpha II spectrin and actin levels were determined by immunoblot analysis. (*Right*) Quantification of cleaved spectrin is shown (each group $n = 10$, $*P < 0.05$). (*B*) WFS1 mRNA levels in different parts of brain in WFS1$^{-/-}$ and WFS1$^{+/-}$ mice were measured by qRT-PCR. (*C*) Two-dimensional fluorescence difference gel electrophoresis of cerebellum proteins from WFS1 knockout (WFS1$^{-/-}$, labeled in red) and control (WFS1$^{+/+}$, labeled in green) mice showing common (Merge, labeled in yellow) and unique proteins (circled). (*D*) The protein expression ratios between WFS1 knockout and control mice were generated, and differentially expressed spots were analyzed by MALDI-TOF mass spectrometry. Quantitative diagrams of spots #2 and #3, identified by mass spectrometry as myelin basic protein, showing lower levels of expression in WFS1 knockout mice compared with control mice. (*E*) Protein was extracted from cerebellums of WFS1 brain-specific knockout (−/−) and control (+/+) mice. Cleaved myelin basic protein (black arrow), cleaved spectrin, WFS1 and GAPDH levels were determined by immunoblot analysis (left panel) and quantified in the right panel (each group $n = 3$, $*P < 0.05$).

calpain activation and cell death in WFS1-knockdown NSC34 cells (Fig. 6*E*). To verify these observations in patient cells, we pre-treated neural progenitor cells derived from iPSCs of a Wolfram syndrome patient and an unaffected parent with dantrolene, and then challenged these cells with thapisgargin. Thapsigargin-induced cell death was increased in neural progenitor cells derived from the

Wolfram syndrome patient relative to those derived from the un-affected parent, and dantrolene could prevent cell death in the patient iPSC-derived neural progenitor cells (Fig. 6*F*). In addition, we treated brain-specific WFS1 knockout mice with dantrolene and observed evidence of suppressed calpain activation in brain lysates from these mice (Fig. 6*G*). Collectively, these results argue
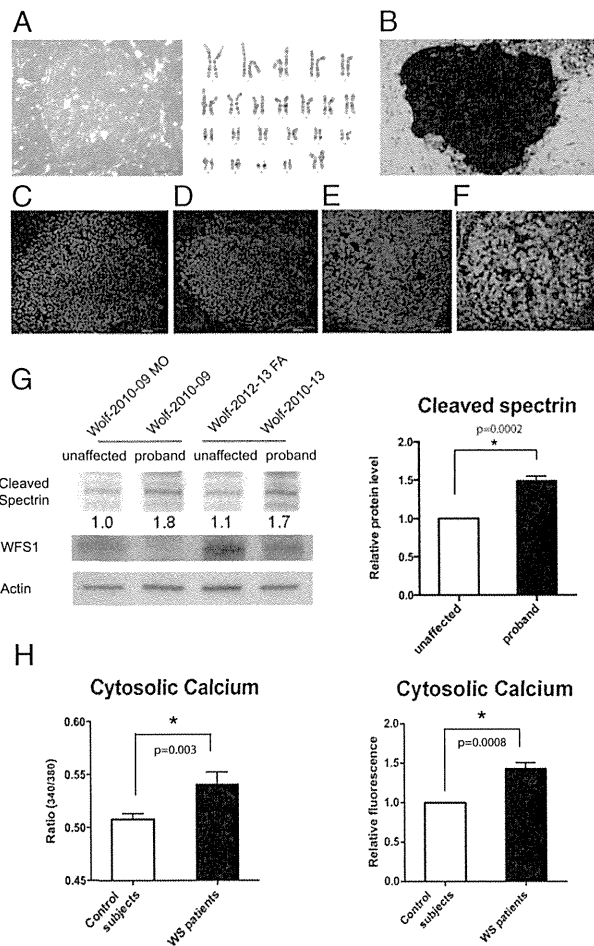
Fig. 5. High cytosolic calcium levels and hyperactivation of calpain in patient neural progenitor cells. (*A, Left*) Wolfram syndrome iPS cells derived from fibroblasts of a patient 1610. (*A, Right*) Karyotype of the Wolfram iPS cells. (*B*) Alkaline phosphatase staining of the Wolfram iPS cells. (*C–F*) Wolfram syndrome iPS cells stained with pluripotent markers: Nanog (*C*), Sox2 (*D*), SSEA4 (*E*), and TRA-1 (*F*). (*G*) Immunoblot analysis of cleaved spectrin and actin in neural progenitor cells derived from Wolfram syndrome patient iPS cells. The relative levels of the spectrin cleavage product are indicated (*Left*) and quantified (*Right*) ($n = 4$, *$P < 0.05$). (*H, Left*) Quantitative analysis of cytosolic calcium levels in unaffected controls and Wolfram syndrome patients measured by Fura-2 calcium indicator (All values are means ± SEM; experiment was performed six independent times with >3 wells per sample each time; $n = 6$, *$P < 0.05$). (*H, Right*) Quantification of cytosolic calcium levels in unaffected controls and Wolfram syndrome patients measured by Fluo-4 calcium assay (experiment was performed four independent times; $n = 4$, *$P < 0.05$).

that dantrolene could prevent cell death in Wolfram syndrome by suppressing calpain activation.

Discussion

Growing evidence indicates that ER dysfunction triggers a range of human chronic diseases, including diabetes, atherosclerosis, inflammatory bowel disease, and neurodegenerative diseases (3, 4, 37–39). However, currently there is no effective therapy targeting the ER for such diseases due to the lack of clear understanding of the ER's contribution to the pathogenesis of these diseases. Although Wolfram syndrome is a rare disease and therefore not a focus of drug discovery efforts, the homogeneity of the patient population and disease mechanism has enabled us

to identify a potential target, a calcium-dependent protease, calpain. Our results provide new insights into how the pathways leading to calpain activation cause β cell death and neurodegeneration, which are schematically summarized in Fig. 6*H*.

There are two causative genes for Wolfram syndrome, *WFS1* and *WFS2*. The functions of WFS1 have been extensively studied in pancreatic β cells. It has been shown that WFS1-deficient pancreatic β cells have high baseline ER stress levels and impaired insulin synthesis and secretion. Thus, WFS1-deficient β cells are susceptible to ER stress mediated cell death (5, 6, 32, 40–42). The functions of WFS2 are still not clear. There is evidence showing that impairment of WFS2 function can cause neural atrophy, muscular atrophy, and accelerate aging in mice (14). WFS2 has also been shown to be involved in autophagy (43). However, although patients with both genetic types of Wolfram syndrome suffer from the same disease manifestations, it was not clear if a common molecular pathway was altered in these patients. Our study has demonstrated, to our knowledge for the first time, that calpain hyperactivation is the common molecular pathway altered in patients with Wolfram syndrome. The mechanisms of calpain hyperactivation are different in the two genetic types of Wolfram syndrome. WFS1 mutations cause calpain activation by increasing cytosolic calcium levels, whereas WFS2 mutations lead to calpain activation due to impaired calpain inhibition.

Previously, Wolfram syndrome studies focused on pancreatic β cell function (5, 40, 41). However, patients also suffer from neuronal manifestations. MRI scans of Wolfram syndrome patients showed atrophy in brain tissue implying neurodegeneration in patients (7, 10). To investigate the mechanisms of neurodegeneration in Wolfram syndrome human cells, we established Wolfram syndrome iPSC-derived neural progenitor lines and confirmed the observations found in rodent cells and animal models of Wolfram syndrome. Differentiation of these iPSC-derived neural progenitor cells into specific types of neurons should be carried out in the future to better understand which cell types are damaged in Wolfram syndrome; this will lead to a better understanding of the molecular basis of this disease and provide cell models for future drug development.

Calpain activation has been found to be associated with type 2 diabetes and various neuronal diseases including Alzheimers, traumatic brain injury and cerebral ischemia, suggesting that regulation of calpains is crucial for cellular health (23). We discovered that calpain inhibitor III could confer protection against thapsigargin mediated cell death (Fig. 6*A*). Our data also demonstrates that calpeptin treatment was beneficial for cells with impaired WFS2 function. These results suggest that targeting calpain could be a novel therapeutic strategy for Wolfram syndrome. However, calpain is also an essential molecule for cell survival (44). Controlling calpain activation level is a double-bladed sword. We should carefully monitor calpain functions in treating patients with Wolfram syndrome (44).

Calpain activation is tightly regulated by cytosolic calcium levels. In other syndromes that increase cytosolic calcium level in pancreatic β cells, patients experience a transient or permanent period of hyperinsulinaemic hypoglycemia. This hyperinsulinaemic hypoglycemia can be partially restored by an inhibitor for ATP-sensitive potassium (K_{ATP}) channels or a calcium channel antagonist that prevents an increase in cytosolic calcium levels (45, 46). Although patients with Wolfram syndrome do not experience a period of hyperinsulinaemic hypoglycemia, small molecule compounds capable of altering cellular calcium levels may prevent calpain 2 activation and hold promise for treating patients with Wolfram syndrome. Treatment of WFS1-knockdown cells with dantrolene and ryanodine could prevent cell death mediated by WFS1 knockdown. Dantrolene is a muscle relaxant drug prescribed for multiple sclerosis, cerebral palsy or malignant hyperthermia (47). Dantrolene inhibits the ryanodine receptors and
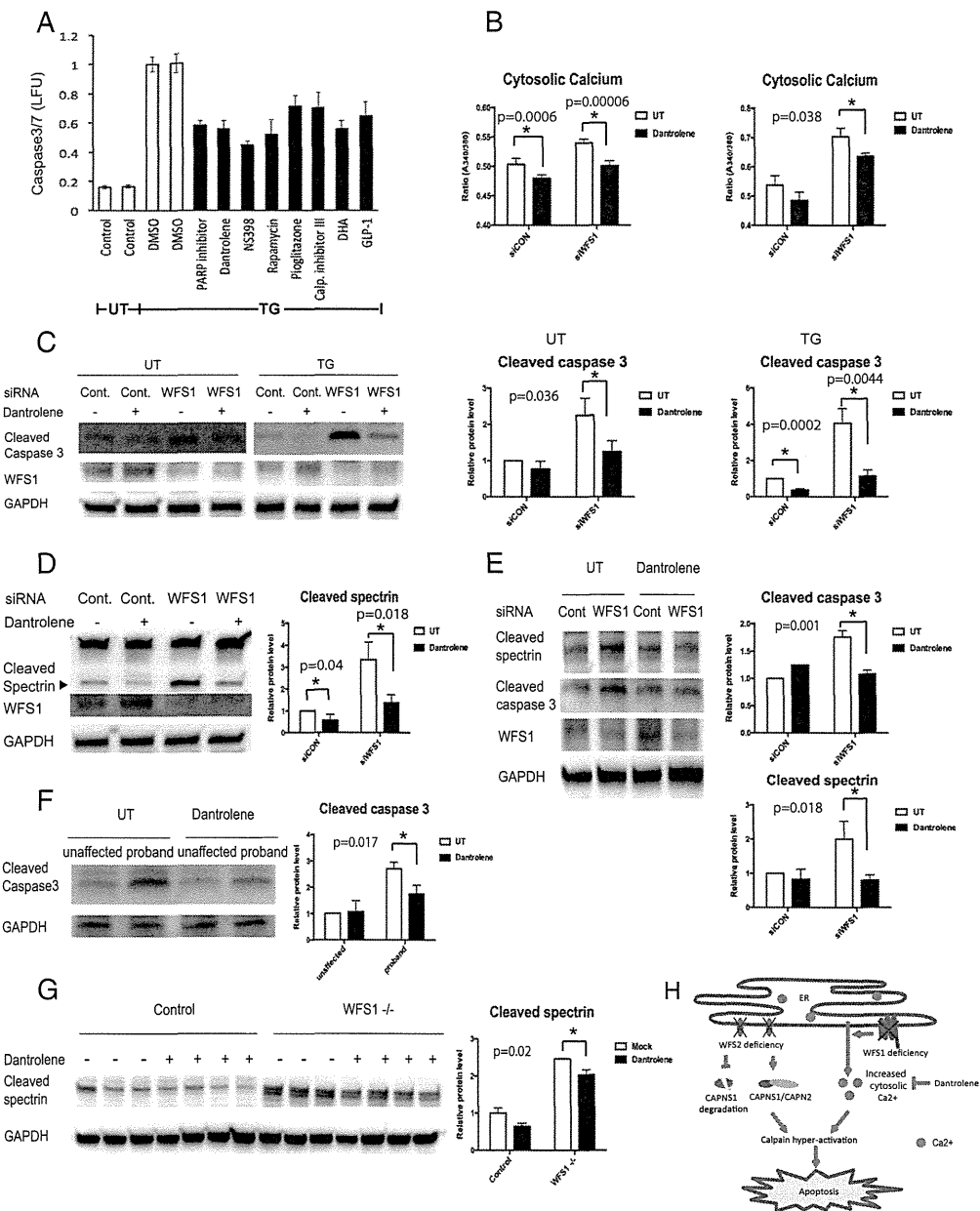
Fig. 6. Dantrolene prevents cell death in iPS cell-derived neural progenitor cells of Wolfram syndorme by inhibiting the ER calcium leakage to the cytosol. (A) INS-1 832/13 cells were pretreated with DMSO or drugs for 24 h then incubated in media containing 20 nM of thapsigargin (TG) overnight. Apoptosis was detected by caspase 3/7-Glo luminescence. (B) Cytosolic calcium levels were determined by Fura-2 in control and WFS1-deficient INS-1 832/13 (Left) and NSC34 (Right) cells treated or untreated with 10 µM dantrolene for 24 h (All values are means ± SEM; experiment was performed 6 independent times with >3 wells per sample each time $n = 6$, *$P < 0.05$). (C) INS-1 832/13 cells were transfected with scrambled siRNA or siRNA against WFS1. Cells were pretreated with or without 10 µM dantrolene for 48 h, then incubated in media with or without 0.5 µM TG for 6 h. Expression levels of cleaved caspase-3, WFS1, GAPDH were measured by immunoblotting (Left). Protein levels of caspase3 under untreated (Center) and TG treated (Right) conditions are quantified and shown as bar graphs ($n = 3$, *$P < 0.05$). (D) INS-1 832/13 cells were transfected with scrambled siRNA or siRNA against WFS1, pretreated with or without 10 µM dantrolene for 48 h, then incubated in media containing 0.5 µM TG for 6 h. Protein levels of cleaved spectrin, WFS1, GAPDH were analyzed by immunoblotting (Left) and quantified (Right) ($n = 3$, *$P < 0.05$). (E) NSC34 cells were transfected with scrambled siRNA or siRNA against WFS1. Then treated with or without10 µM dantrolene for 24 h. Protein levels of cleaved spectrin, cleaved caspase 3, WFS2 and GAPDH were determined by immunoblotting (Left) and quantified (Right) ($n = 3$, *$P < 0.05$). (F) Wolfram patient neural progenitor cells were pretreated with or without 10 µM dantrolene for 48 h. Then, cells were treated with 0.125 µM TG for 20 h. (Left) Apoptosis was monitored by immunoblotting. (Right) Quantification of cleaved caspase 3 protein levels are indicated ($n = 3$, *$P < 0.05$). (G) Control and WFS1 brain-specific knockout mice were treated with water or dantrolene for 4 wk at 20 mg/kg. Brain lysates of these mice were examined by immunoblotting. Protein levels of cleaved spectrin and GAPDH were monitored (Left) and quantified (Right) (All values are means ± SEM; each group $n > 3$, *$P < 0.05$). (H) Scheme of the pathogenesis of Wolfram syndrome.

Lu et al.

reduces calcium leakage from the ER to cytosol, lowering cytosolic calcium level. The protective effect of dantrolene treatment on WFS1-deficient cells suggests that dysregulated cellular calcium homeostasis plays a role in the disease progression of Wolfram syndrome. In addition, it has been shown that stabilizing ER calcium channel function could prevent the progression of neurodegeneration in a mouse model of Alzheimer's disease (48). Therefore, modulating calcium levels may be an effective way to treat Wolfram syndrome or other ER diseases.

Dantrolene treatment did not block cell death mediated by WFS2 knockdown, suggesting that WFS2 does not directly affect the ER calcium homeostasis (Fig. S4 *D* and *E*). RNAi-mediated WFS1 knockdown in HEK293 cells significantly reduced the activation levels of sarco/endoplasmic reticulum calcium transport ATPase (SERCA), indicating that WFS1 may play a role in the modulation of SERCA activation and ER calcium levels (Fig. S5). It has been shown that WFS1 interacts with the Na^+/K^+ ATPase $\beta 1$ subunit and the expression of WFS1 parallels that of Na^+/K^+ ATPase $\beta 1$ subunit in a variety of settings, suggesting that WFS1 may function as an ion channel or regulator of existing channels (42). Further studies on this topic would be necessary to completely understand the etiology of Wolfram syndrome.

Our study reveals that dantrolene can prevent ER stress-mediated cell death in human and rodent cell models as well as mouse models of Wolfram syndrome. Thus, dantrolene and other drugs that regulate ER calcium homeostasis could be used to delay the progression of Wolfram syndrome and other diseases associated with ER dysfunction, including type 1 and type 2 diabetes.

Materials and Methods

Human Subjects. Wolfram syndrome patients were recruited through the Washington University Wolfram Syndrome International Registry website (wolframsyndrome.dom.wustl.edu). The clinic protocol was approved by the Washington University Human Research Protection Office and all subjects provided informed consent if adults and assent with consent by parents if minor children (IRB ID 201107067 and 201104010).

Animal Experiments. WFS1 brain-specific knockout mice were generated by breeding the Nestin-Cre transgenic mice (Jackson Laboratory) with WFS1 floxed mice (40). WFS2 whole body knockout mice are purchased from MRC Harwell. All animal experiments were performed according to procedures approved by the Institutional Animal Care and Use Committee at the Washington University School of Medicine (A-3381-01).

Calcium Levels. Calcium levels in cells were measured by Fura-2 AM dye and Fluo-4 AM dye (Life Technology) Inifinite M1000 (Tecan). Cells were plated in 96-well plates at 25,000 cells per well and stained with 4 μg/mL Fura-2 dye along with 2.5 mM probenecid for 30 min, then the cells were washed with PBS and kept in the dark for another 30 min to allow cleavage of AM ester. Fluorescence was measured at excitation wavelength 510 nm and emission wavelengths 340 nm and 380 nm. Then background subtractions were performed with both emission wavelengths. The subtraction result was used to calculate 340/380 ratios.

For Fluo-4 AM staining, neural progenitor cells were plated in 24-well plates at 200,000 cells per well. After staining with Fluo-4 AM dye for 30 min along with 2.5 mM probenecid, cells were washed and resuspended in PBS. Incubation for a further 30 min was performed to allow complete deesterification of intracellular AM esters. Then, samples were measured by flow cytometry at the FACS core facility of Washington University School of Medicine using a LSRII instrument (BD). The results were analyzed by FlowJo ver.7.6.3.

Statistical Analysis. Two-tailed *t* tests were used to compare the two treatments. *P* values below 0.05 were considered significant. All values are shown as means ± SD if not stated. Please see *SI Materials and Methods* for complete details.

1. Ron D, Walter P (2007) Signal integration in the endoplasmic reticulum unfolded protein response. *Nat Rev Mol Cell Biol* 8(7):519–529.
2. Tabas I, Ron D (2011) Integrating the mechanisms of apoptosis induced by endoplasmic reticulum stress. *Nat Cell Biol* 13(3):184–190.
3. Hetz C, Chevet E, Harding HP (2013) Targeting the unfolded protein response in disease. *Nat Rev Drug Discov* 12(9):703–719.
4. Wang S, Kaufman RJ (2012) The impact of the unfolded protein response on human disease. *J Cell Biol* 197(7):857–867.
5. Fonseca SG, et al. (2005) WFS1 is a novel component of the unfolded protein response and maintains homeostasis of the endoplasmic reticulum in pancreatic beta-cells. *J Biol Chem* 280(47):39609–39615.
6. Fonseca SG, et al. (2010) Wolfram syndrome 1 gene negatively regulates ER stress signaling in rodent and human cells. *J Clin Invest* 120(3):744–755.
7. Barrett TG, Bundey SE, Macleod AF (1995) Neurodegeneration and diabetes: UK nationwide study of Wolfram (DIDMOAD) syndrome. *Lancet* 346(8988):1458–1463.
8. Wolfram DJ, Wagener HP (1938) Diabetes mellitus and simple optic atrophy among siblings: Report of four cases. *Mayo Clin Proc* 1:715–718.
9. Urano F (2014) Diabetes: Targeting endoplasmic reticulum to combat juvenile diabetes. *Nat Rev Endocrinol* 10(3):129–130.
10. Hershey T, et al.; Washington University Wolfram Study Group (2012) Early brain vulnerability in Wolfram syndrome. *PLoS ONE* 7(7):e40604.
11. Marshall BA, et al.; Washington University Wolfram Study Group (2013) Phenotypic characteristics of early Wolfram syndrome. *Orphanet J Rare Dis* 8(1):64.
12. Inoue H, et al. (1998) A gene encoding a transmembrane protein is mutated in patients with diabetes mellitus and optic atrophy (Wolfram syndrome). *Nat Genet* 20(2):143–148.
13. Amr S, et al. (2007) A homozygous mutation in a novel zinc-finger protein, ERIS, is responsible for Wolfram syndrome 2. *Am J Hum Genet* 81(4):673–683.
14. Chen YF, et al. (2009) Cisd2 deficiency drives premature aging and causes mitochondria-mediated defects in mice. *Genes Dev* 23(10):1183–1194.
15. Wiley SE, et al. (2013) Wolfram Syndrome protein, Miner1, regulates sulphydryl redox status, the unfolded protein response, and Ca2+ homeostasis. *EMBO Mol Med* 5(6):904–918.
16. Shang L, et al. (2014) β-cell dysfunction due to increased ER stress in a stem cell model of Wolfram syndrome. *Diabetes* 63(3):923–933.
17. Sandhu MS, et al. (2007) Common variants in WFS1 confer risk of type 2 diabetes. *Nat Genet* 39(8):951–953.
18. Bonnycastle LL, et al. (2013) Autosomal dominant diabetes arising from a Wolfram syndrome 1 mutation. *Diabetes* 62(11):3943–3950.
19. Goll DE, Thompson VF, Li H, Wei W, Cong J (2003) The calpain system. *Physiol Rev* 83(3):731–801.
20. Tan Y, et al. (2006) Ubiquitous calpains promote caspase-12 and JNK activation during endoplasmic reticulum stress-induced apoptosis. *J Biol Chem* 281(23):16016–16024.
21. Tan Y, Wu C, De Veyra T, Greer PA (2006) Ubiquitous calpains promote both apoptosis and survival signals in response to different cell death stimuli. *J Biol Chem* 281(26):17689–17698.
22. Nakagawa T, Yuan J (2000) Cross-talk between two cysteine protease families. Activation of caspase-12 by calpain in apoptosis. *J Cell Biol* 150(4):887–894.
23. Cui W, et al. (2013) Free fatty acid induces endoplasmic reticulum stress and apoptosis of β-cells by Ca2+/calpain-2 pathways. *PLoS ONE* 8(3):e59921.
24. Huang CJ, et al. (2010) Calcium-activated calpain-2 is a mediator of beta cell dysfunction and apoptosis in type 2 diabetes. *J Biol Chem* 285(1):339–348.
25. Barrett TG, Bundey SE (1997) Wolfram (DIDMOAD) syndrome. *J Med Genet* 34(10):838–841.
26. Liu MC, et al. (2006) Comparing calpain- and caspase-3-mediated degradation patterns in traumatic brain injury by differential proteome analysis. *Biochem J* 394(Pt 3):715–725.
27. Hara T, et al. (2014) Calcium efflux from the endoplasmic reticulum leads to β-cell death. *Endocrinology* 155(3):758–768.
28. Takei D, et al. (2006) WFS1 protein modulates the free Ca(2+) concentration in the endoplasmic reticulum. *FEBS Lett* 580(24):5635–5640.
29. Liu MC, et al. (2006) Extensive degradation of myelin basic protein isoforms by calpain following traumatic brain injury. *J Neurochem* 98(3):700–712.
30. Takahashi K, Yamanaka S (2006) Induction of pluripotent stem cells from mouse embryonic and adult fibroblast cultures by defined factors. *Cell* 126(4):663–676.
31. Yusta B, et al. (2006) GLP-1 receptor activation improves beta cell function and survival following induction of endoplasmic reticulum stress. *Cell Metab* 4(5):391–406.
32. Akiyama M, et al. (2009) Increased insulin demand promotes while pioglitazone prevents pancreatic beta cell apoptosis in Wfs1 knockout mice. *Diabetologia* 52(4):653–663.
33. Bachar-Wikstrom E, et al. (2013) Stimulation of autophagy improves endoplasmic reticulum stress-induced diabetes. *Diabetes* 62(4):1227–1237.
34. Dykes MH (1975) Evaluation of a muscle relaxant: Dantrolene sodium (Dantrium). *JAMA* 231(8):862–864.

35. Wei H, Perry DC (1996) Dantrolene is cytoprotective in two models of neuronal cell death. *J Neurochem* 67(6):2390–2398.
36. Luciani DS, et al. (2009) Roles of IP3R and RyR Ca2+ channels in endoplasmic reticulum stress and beta-cell death. *Diabetes* 58(2):422–432.
37. Hotamisligil GS (2010) Endoplasmic reticulum stress and atherosclerosis. *Nat Med* 16(4):396–399.
38. Hotamisligil GS (2010) Endoplasmic reticulum stress and the inflammatory basis of metabolic disease. *Cell* 140(6):900–917.
39. Ozcan L, Tabas I (2012) Role of endoplasmic reticulum stress in metabolic disease and other disorders. *Annu Rev Med* 63:317–328.
40. Riggs AC, et al. (2005) Mice conditionally lacking the Wolfram gene in pancreatic islet beta cells exhibit diabetes as a result of enhanced endoplasmic reticulum stress and apoptosis. *Diabetologia* 48(11):2313–2321.
41. Ishihara H, et al. (2004) Disruption of the WFS1 gene in mice causes progressive beta-cell loss and impaired stimulus-secretion coupling in insulin secretion. *Hum Mol Genet* 13(11):1159–1170.
42. Zatyka M, et al. (2008) Sodium-potassium ATPase 1 subunit is a molecular partner of Wolframin, an endoplasmic reticulum protein involved in ER stress. *Hum Mol Genet* 17(2):190–200.
43. Chang NC, Nguyen M, Germain M, Shore GC (2010) Antagonism of Beclin 1-dependent autophagy by BCL-2 at the endoplasmic reticulum requires NAF-1. *EMBO J* 29(3): 606–618.
44. Dutt P, et al. (2006) m-Calpain is required for preimplantation embryonic development in mice. *BMC Dev Biol* 6:3.
45. Arya VB, Mohammed Z, Blankenstein O, De Lonlay P, Hussain K (2014) Hyper-insulinaemic hypoglycaemia. *Hormone Metabolic Res* 46(3):157–170.
46. Shah P, Demirbilek H, Hussain K (2014) Persistent hyperinsulinaemic hypoglycaemia in infancy. *Semin Pediatr Surg* 23(2):76–82.
47. Krause T, Gerbershagen MU, Fiege M, Weisshorn R, Wappler F (2004) Dantrolene—a review of its pharmacology, therapeutic use and new developments. *Anaesthesia* 59(4):364–373.
48. Chakroborty S, et al. (2012) Stabilizing ER Ca2+ channel function as an early preventative strategy for Alzheimer's disease. *PLoS ONE* 7(12):e52056.

Lu et al.

— 237 —

MINI REVIEW

Generation of pluripotent stem cells without the use of genetic material

Akon Higuchi[1,2,9], Qing-Dong Ling[3,4,9], S Suresh Kumar[5], Murugan A Munusamy[2], Abdullah A Alarfaj[2], Yung Chang[6], Shih-Hsuan Kao[1], Ke-Chen Lin[1], Han-Chow Wang[7] and Akihiro Umezawa[8]

Induced pluripotent stem cells (iPSCs) provide a platform to obtain patient-specific cells for use as a cell source in regenerative medicine. Although iPSCs do not have the ethical concerns of embryonic stem cells, iPSCs have not been widely used in clinical applications, as they are generated by gene transduction. Recently, iPSCs have been generated without the use of genetic material. For example, protein-induced PSCs and chemically induced PSCs have been generated by the use of small and large (protein) molecules. Several epigenetic characteristics are important for cell differentiation; therefore, several small-molecule inhibitors of epigenetic-modifying enzymes, such as DNA methyl-transferases, histone deacetylases, histone methyltransferases, and histone demethylases, are potential candidates for the reprogramming of somatic cells into iPSCs. In this review, we discuss what types of small chemical or large (protein) molecules could be used to replace the viral transduction of genes and/or genetic reprogramming to obtain human iPSCs.

Pluripotent stem cells (PSCs) can be derived from terminally differentiated tissues by altering the epigenetic status of cells. These PSCs have the potential to differentiate into any cell type derived from the three germ layers.[1–5] Cell type determination is heavily dependent on epigenetic process. The generation of iPCSs from differentiated cells is partly regulated by epigenetics. PSCs provide an unlimited cell source with the potential for use in studying diseases, drug screening, and regenerative medicine. Human PSCs provide a promising platform for obtaining patient-specific cells for various therapeutic and research applications. In general, induced pluripotent stem cells (iPSCs) are generated via genetic manipulation or by nuclear transfer to generate PSCs from somatic cells.[6] However, nuclear transfer-generated PSCs raised ethical concerns and are technically difficult to prepare. The genetic manipulation of PSCs limits their clinical uses. Although embryonic stem cells (ESCs) do not need to be genetically manipulated, there are strong ethical concerns regarding human ESCs (hESCs), limiting their use in clinical applications.

iPSCs were first generated in 2006–2007 by the transduction of four transcription genes, Oct3/4, Sox2, c-Myc, and Klf-4[7–10] or Oct 4, Sox2, Nanog, and Lin28.[11] Following these studies, several researchers succeeded in generating iPSCs using fewer pluripotent genes. Of note, researchers generated iPSCs without transducing c-Myc, a potent oncogene.[12–14] Currently, mouse iPSCs (miPSCs) can be generated by reprogramming a single gene, such as Oct4,[15,16] or with the aid of small or large molecules in place of gene transduction.[17–19] However, the low reprogramming efficiency of human iPSCs (hiPSCs) is a major drawback. The use of virus-mediated delivery of reprogramming factors, which leads to the permanent integration of oncogenes and potentially harmful genomic alterations,[20] is a serious concern. The use of genome-integrating viruses could cause insertional mutagenesis and unpredictable genetic dysfunction.[9,21]

Therefore, several reprogramming technologies that do not use viral integration have been developed for iPSC production.[22,23] These approaches include the use of non-integrating viruses,[24–26] transposon-based systems,[27] and the delivery of reprogramming factors on plasmids.[22,28–30] Adenovirus, lentivirus, Sendai virus, miRNA, and plasmid transfection methods have been reported to generate miPSCs[28,31] and

[1]Department of Chemical and Materials Engineering, National Central University, Jhongli, Taiwan; [2]Department of Botany and Microbiology, King Saud University, Riyadh, Saudi Arabia; [3]Institute of Systems Biology and Bioinformatics, National Central University, Jhongli, Taiwan; [4]Cathay Medical Research Institute, Cathay General Hospital, Taipei, Taiwan; [5]Department of Medical Microbiology and Parasitology, Universities Putra Malaysia, Slangor, Malaysia; [6]Department of Chemical Engineering, R&D Center for Membrane Technology, Chung Yuan Christian University, Jhongli, Taiwan; [7]Department of Obstetrics and Gynecology, Hungchi Women and Children's Hospital, Jhongli, Taiwan and [8]Department of Reproduction, National Research Institute for Child Health and Development, Tokyo, Japan
Correspondence: Professor A Higuchi, PhD, Department of Chemical and Materials Engineering, National Central University, No. 300, Jhongda Road, Jhongli 32001, Taiwan.
E-mail: higuchi@ncu.edu.tw
[9]These authors contributed equally to this work.

hiPSCs[24,30,32-35] to minimize chromosomal disruption.[18] Yu *et al.* generated hiPSCs by transfecting non-integrating episomal vectors.[30] In addition, the piggyBac transposon[18,27,31] and Cre-recombinase excisable viruses[36] have been used to generate hiPSCs. The transgenes can be excised by inducible gene expression once reprogramming is established.[25,27,36] However, there is evidence that there can be problems with residual DNA and chromosomal disruptions, resulting in harmful genetic alterations.[18]

The repeated transfection of modified mRNA encoding the reprogramming factors is also efficient for generating iPSCs.[22,37] Although these strategies eliminate the threat of random viral integration into the host cell genome, these approaches are technically challenging and less efficient than viral transduction. Therefore, it is important to identify new conditions and small or large molecules that can promote reprogramming and ultimately replace all of the reprogramming transcription factors (TFs).[14,38-41] For clinical applications, using small or large molecules to generate PSCs are preferable to genetic manipulations. Recently, several novel methods have been reported for generation of iPSCs without the use of genetic material; these methods include protein-induced PSCs (piPSCs) that are reprogrammed from somatic cells using cell-penetrating TF proteins,[18,19] and chemically iPSCs (CiPSCs) that are reprogrammed from somatic cells using small molecules.[14,17,20,38-49]

Human CiPSCs are a promising tool in the clinical application of PSCs. CiPSCs can be reprogrammed to become iPSCs from somatic cells, without genetic manipulation, through the addition of small-molecule chemicals in the culture medium. In this review, we will discuss the generation of iPSCs without the use of genetic material and instead using small or large (protein) molecules. We will discuss types of small and/or large (protein) molecules that can replace specific viral transduction of pluripotent TFs to obtain piPSCs and CiPSCs from somatic cells.

PSCs REPROGRAMMING WITH PROTEINS (piPSCs)

In the reprogramming of somatic cells into iPSCs, one of the methods that avoids exogenous genetic introduction to the target cells is delivering the reprogramming proteins directly into cells rather than transducing the cells with TF genes. Previous researchers have reported that the proteins can be delivered into mammalian cells *in vitro* and *in vivo* by conjugating the proteins with a short peptide to guide their transduction, such as HIV transactivator of transcription (tat) or polyarginine.[30,50-52] Various solubilization and refolding techniques have been developed so that recombinant proteins expressed in *E. coli* and contained in inclusion bodies can be re-folded into bioactive proteins. This allows for easy, large-scale production of therapeutic proteins.[30,53] Currently, recombinant forms of Oct4, Sox2, Klf4, and c-Myc are commercially available. Table 1 summarizes the reprogramming of mouse and human somatic cells into piPSCs with the aid of proteins by transduction without TFs.

The challenge in delivering proteins into cells is the proteins' limited capacity to penetrate the cell membranes. Proteins that are capable of crossing the cell membrane barrier generally contain high proportions of basic amino acids, such as lysine and arginine.[54,55] and the HIV tat protein has a short, basic segment of 48-60 amino-acid residues that is known to cross the cell membrane and to activate HIV-specific genes.[18,54] In 2009, Zhou *et al.* attached a transfection domain of a polyarginine protein to the C terminus of the four reprogramming factors Oct4, Sox2, Klf4, and c-Myc to generate recombinant proteins that are able to permeate the plasma membranes of mouse embryonic fibroblasts (MEFs).[19] The mouse piPSCs that were generated were stably expanded for 30 passages, and the morphology of the piPSCs was similar to ESCs, as they formed small, compact, domed colonies.[19] The piPSCs expressed typical pluripotency markers, including ALP, SSEA1, Nanog, Oct4, and Sox2, as assayed by immunostaining. The expression of endogenous pluripotency genes was verified by RT-PCR. The piPSCs generated embryoid bodies in suspension and differentiated into cells characteristic of the three germ layers: (a) endoderm cells expressing AFP, FoxA2, GATA4, Sox17, albumin (hepatic marker), and Pdx1 (pancreatic marker); (b) mesoderm cells expressing Brachyury and mature beating cardiomyocytes expressing the CT3 and MHC markers; and (c) ectoderm cells expressing Pax5 and Sox1 (neural markers) and *β*III-tubulin and MAP2ab (mature neuronal markers).[19] Although these findings are promising, the extremely low efficiency (0.006%) and poor reproducibility of the generation of piPSCs hinders its use as a general method for generating iPSCs.

The same year, Kim *et al.* reported the generation of piPSCs from human newborn fibroblasts (HNFs) using four recombinant cell-penetrating reprogramming proteins (Oct4, Sox2, Klf4, and c-Myc) fused with a cell-penetrating peptide (CPP, polyarginine with nine repeating arginine residues).[18] The authors generated HEK293 cell lines that expressed each of the four human reprogramming proteins fused to CPP. HNFs were treated with cell extracts from the HEK293 cell lines. After repeated treatment with the cell extracts containing the reprogramming proteins, the HNFs ultimately became human piPSCs.[18] The human piPSCs showed similar characteristics to hESCs (H9) in cell morphology and pluripotent marker expression and were cultured for more than 35 passages without loss of pluripotency, which suggests that the appropriate epigenetic reprogramming events occurred in these cells. The human piPSCs were successively differentiated into cells derived from the three germ layers both *in vitro* (embryonic formation) and *in vivo* (teratoma formation).[18] Interestingly, Kim *et al.* could not generate mouse piPSCs when they applied the same method to mouse cells.[18] This discrepancy might be due to a low concentration of reprogramming proteins, as they used whole-protein extracts from HEK293 cells as the source of the reprogramming proteins. Furthermore, Kim *et al.* did not add

— 239 —